Atmos. Chem. Phys. Discuss., 15, 26895–26957, 2015
www.atmos-chem-phys-discuss.net/15/26895/2015/
doi:10.5194/acpd-15-26895-2015
© Author(s) 2015. CC Attribution 3.0 License.

Atmospheric Chemistry and Physics Discussions
Open Access

This discussion paper is/has been under review for the journal Atmospheric Chemistry and Physics (ACP). Please refer to the corresponding final paper in ACP if available.

Decadal-scale relationship between measurements of aerosols, land-use change, and fire over Southeast Asia

J. B. Cohen and E. Lecoeur

National University of Singapore, Department of Civil and Environmental Engineering, 1 Engineering Drive 2, E1A #07-03, 117576, Singapore

Received: 8 August 2015 – Accepted: 7 September 2015 – Published: 6 October 2015

Correspondence to: J. B. Cohen (jasonbc@alum.mit.edu)

Published by Copernicus Publications on behalf of the European Geosciences Union.

CC BY

Abstract

A simultaneous analysis of 13 years of remotely sensed data of land cover, fires, precipitation, and aerosols from the MODIS, TRMM, and MISR satellites and the AERONET network over Southeast Asia is performed, leading to a set of robust relationships between land-use change and fire being found on inter-annual and intra-annual scales over Southeast Asia, reflecting the heavy amounts of anthropogenic influence over land use change and fires in this region of the world. First, we find that fires occur annually, but with a considerable amount of variance in their onset, duration, and intensity from year to year, and from two separate regions within Southeast Asia from each other. This variability is already partially understood from previous works, including the impacts of both inter-annually and intra-annually occurring influences such as the Monsoon and El-Nino events, but yet there are other as of yet unknown influences that also are found to strongly influence the results. Second, we show that a simple regression-model of the land-cover, fire, and precipitation data can be used to recreate a robust representation of the timing and magnitude of measured AOD from multiple measurements sources of this region using either 8-day (better for onset and duration) or monthly based (better for magnitude) measurements, but not daily measurements. We find that the reconstructed AOD matches the timing and intensity from AERONET measurements to within 70 to 90 % and the timing and intensity of MISR measurements from to within 50 to 95 %. This is a unique finding in this part of the world, since could-covered regions are large, yet the robustness of the model is still capable of holding over many of these regions, where otherwise no fires are observed and hence no emissions source contribution to AOD would otherwise be thought to occur. Third, we determine that while Southeast Asia is a source region of such intense smoke emissions, that it is also impacted by transport of smoke from other regions as well. There are regions in northern Southeast Asia which have two annual AOD peaks, one during the local fire season, and the second smaller peak corresponding to a combination of some local smoke sources as well as transport of aerosols from fires in southern

ACPD
15, 26895–26957, 2015

CC BY

Southeast Asia, and possibly even from anthropogenic sources in South Asia. Conversely, we show that southern Southeast Asia is affected exclusively by its own local fire sources during its own local fire season. Overall, this study highlights the importance of taking into account a simultaneous use of land-use, fire, and precipitation for understanding the impacts of fires on the atmospheric loading and distribution of aerosols in Southeast Asia over both space and time.

1 Introduction

Southeast Asia has been experiencing major haze events over the past three to five decades, due to a combination of increased urbanization (Cohen and Wang, 2014; Cohen and Prinn, 2011) and large-scale conversion of forests by fire (Cohen, 2014; van der Werf et al., 2008; Taylor, 2010; Dennis, 2005). The underlying connections and mechanisms relating the sources and strength of fire-based emissions and observed intra-annual, inter-annual, and inter-decadal variations of fire events, with meteorology, land-use change, and anthropogenic driving factors are not well understood (van der Werf et al., 2006; Giglio et al., 2006; Hansen et al., 2008; Field et al., 2009). Moreover, recent studies have shown that the impacts these events have on the atmospheric loading of aerosols and the larger climate are becoming greater in both absolute terms and frequency (Langmann et al., 2009; Nakajima et al., 1999; Podgorny et al., 2003; Rosenfeld, 1999). Some of the heaviest events, which previously in the literature were only associated only with strong El-Nino induced drying events, are now being found to occur in connection with other, less extreme impacts on precipitation and even surface moisture, occurring at various scales including but not limited to the Indian Ocean Dipole, the Madden–Julian Oscillation, the shifting of the Inter-Tropical Conversion Zone, mountain induced waves, the land–sea breeze and localized convection (Fuller and Murphy, 2006; Wooster et al., 2012; Hasler et al., 2009; Reid et al., 2013). The fact that so many factors are capable of influencing these large-scale events is likely to make prediction much more challenging, as is seen by the fact that since

ACPD
15, 26895–26957, 2015

J. B. Cohen and E. Lecoeur

CC BY

2000, there were extreme events, of varying intensity, length, and duration, occurring in 2002, 2004, 2006, 2009, 2013, and 2014 in southern Southeast Asia and every year except 2003 in northern Southeast Asia (Neale and Slingo, 2003; Chang et al., 2005; Aldrian et al., 2007; Cohen, 2014; Wooster et al., 2012).

Direct and indirect emissions of aerosols and gases from these fires, such as black carbon (BC), organic carbon (OC), and ozone, play a major role simultaneously in impacting human health (Afroz et al., 2003), atmospheric radiative forcing (Wang, 2007; Jacobson, 2001; Ming et al., 2010; Ramanathan and Carmichael, 2008; Cohen et al., 2011), and cloud and precipitation properties (Huang et al., 2006; Tao et al., 2012; Wang, 2013). Furthermore, given the general circulation of the Earth, and the lack of precipitation during the dry season in the tropics, coupled with intense localized convection, a large portion of the emitted polutants will have a tendancy to spread widely in space and time, entering into the global-scale circulation patterns (Wang, 2007). Therefore, emissions from these regions during these times of the year may have a significant impact on people and the environment thousands of kilometers away from their source.

One way to quantify the amount of pollution from these events is to estimate the aerosol optical depth (AOD). AOD is a dimensionless variable that defines the proportion of solar radiation that does not reach Earth ground because of scatting and absorption due to aerosols distributed through the atmospheric column. AOD is useful since it can be directly measured by a combination of land-based and space-borne instruments (Holben et al., 1998; Petrenko et al., 2012; Dubovik et al., 2000). The distribution and properties of these aerosols in turn are a function of the initial particulate emissions and gasses from fires and other various anthropogenic sources, in-situ processing, washout from precipitation, and atmospheric transport. Hence, the emissions of primary BC and OC from these fires, coupled with other secondary anthropogenic species, has a one-to-one relationship with a significant change in the AOD, which otherwise would not have occurred over these fire regions and downwind, at these specific times, if the fires were not present.

ACPD
15, 26895–26957, 2015

CC BY

Rapid conversion of forests, agricultural lands, and associated waste products by burning is one of the primary sources of aerosols throughout Southeast Asia (Langmann et al., 2009; Miettinen et al., 2013). However, little is known about the exact spatial and temporal distribution of these fires. Furthermore, the inter-annual and intra-annual variability of biomass burning and its associated underlying mechanisms are also not well understood or constrained by measurements, leading to the current poor understanding of fires impact on the local and global aerosol climatology (van der Werf et al., 2006). Furthermore, Southeastern Asia is often covered with clouds, which further complicates detecting both fire and the pollution that comes from it (Miettinen et al., 2013; Giglio et al., 2006; Remer et al., 2013). A few studies have looked at this and give estimates that the emissions are underestimated, up to a factor of 4 times (Giglio et al., 2003, 2006; Petrenko et al., 2012; Cohen, 2014; Cohen and Wang, 2014).

Given that large-scale fires lead to abrupt and definitive changes in the vegetative properties, we employ a set of measures of land surface properties which have a long time-record, such as LAI (Leaf Area Index), NDVI (Normalized Difference Vegetation Index), and the existence of measured fire (FireMask). While we know that some changes may be masked, obscured, or otherwise missing, any observed abrupt changes in these variables or the land's properties itself must be linked at a minimum with any observed changes in the AOD itself. Moreover, since the onset and the offset on the Asian Monsoon controls the start and end of the fire seasons by rapidly changing from relatively dry to intensely wet and visa versa (Hansen et al., 2008), large scale changes in the monthly-scale precipitation is a proxy for the ability of the fires to occur, as well as washout of aerosols. Therefore, precipitation is also intimately linked with measured AOD over Southeastern Asia.

2 Data and methods

Several remotely sensed and surface measurements of the surface land properties (LAI and NDVI), fires (FireMask), aerosol (AOD), and precipitation (rainfall) are used

ACPD
15, 26895–26957, 2015

CC BY

in this study. These are used in conjunction with advanced analytical procedures to determine the regions which contribute the most to the variance of the impact of fires on the atmosphere loading of aerosols as observed by the AOD. This analysis, in addition to its own results, leads to the production of a simple statistical multi-year constrained model, which is shown to be capable of reproducing the AOD as a function of the land use, fire, and precipitation measurements, even in additional years, and even as tested against measurements of AOD from different sources. All of the details of the measurements used, the procedures and methods employed, and the statistical and analytical techniques employed are detailed below.

2.1 Geography

The domain of interest for this study is Southeast Asia, which we define here as the region spreading from 90 to 130° E in longitude, and from 14° S to 23° N in latitude (see Fig. 3). The subregion defined as northern Southeast Asia is defined by a mostly large continental land masses and a single Wet Season each year, and consists of Thailand, Myanmar, Cambodia, Laos, Vietnam, and parts of southern Greater China and the Phillippines. The subregion defined as southern Southeast Asia is defined by a mixture of land and water and has two Wet Seasons each year, and consists of Malaysia, Indonesia, Brunei, and Singapore.

2.2 Measured Data

For the basic remotely sensed measurements used in the analysis, model construction, and results, we use remotely sensed variables from both the TERRA and AQUA MODIS satellites. Measurements of AOD (Remer et al., 2005) at 0.55 µm consist of both land and ocean pixels, are cloud-cleared, and measured with a daily temporal resolution and a 0.1° by 0.1° spatial resolution. AOD is a measure of the total sunlight light extincted through the atmosphere due to aerosol particles, and therefore is a function of the atmospheric loading of aerosols, washout from precipitation, and the

ACPD
15, 26895–26957, 2015

J. B. Cohen and E. Lecoeur

CC BY

vertical, size, and optical properties of the aerosols. Hence, measured changes in AOD are caused by emissions of aerosols and subsequent in-situ atmospheric processing. It has been shown that strong spatial and temporal variability in AOD measurements over this part of the world, are an expected due to biomass burning in this region of the world, while large measurements of AOD which mostly only co-vary only with precipitation (washout) are more consistent with urban emissions (Cohen, 2014; Cohen and Wang, 2014).

To estimate the land-surface and fire responses we also use the MODIS measured values of LAI, NDVI, and FireMask. MODIS (Nightingale et al., 2008; Yang et al., 2006; Huete et al., 1999; Giglio et al., 2003) measurements of LAI and FireMask are made on an 8-day average basis at 1 km by 1 km horizontal resolution. While for NDVI the measurements are on a 16-day average basis at 1 km by 1 km horizontal resolution. While all three measurements are cloud cleared, optically thin clouds may not be picked up, and this will significantly bias measurements of FireMask, which are inherently based on IR measurements, which could be impaired, while the visible measurements are not impacted.

LAI is chosen since it represents the amount of leaf material in an ecosystem and hence is useful both for indentifying if there was a sudden change in the amount of vegetation available and its condition (Asner et al., 2003), such as expected after leaves are consumed in a fire. It is geometrically defined as the total one-sided area of photosynthetic tissue per unit ground surface area. LAI values range from 0 for bare ground, to the range of 1 to 4 for grassland and crops, to the range of 5 to 9 for plantations, and as high as 10 for dense conifer forests.

NDVI is also chosen since it represents a measure of the health of the vegetation. NDVI is mathematically calculated from the visible (VIS) and near-infrared light reflected (NIR) by the vegetation as follows: $\mathrm{NDVI} = \frac{\mathrm{NIR}-\mathrm{VIS}}{\mathrm{NIR}+\mathrm{VIS}}$. Healthy vegetation absorbs most of the visible light that hits it, and reflects a large portion of the near-infrared light. On the other hand, unhealthy or sparsely healthy vegetation, such as after being burned, reflects more visible light and less near-infrared light. Given this formula,

ACPD
15, 26895–26957, 2015

CC BY

a value close to zero (−0.1 to 0.1) implies that there the land is barren with respect to living and green vegetation, whereas values close to +1.0 correspond to the highest density of healthy green leaves.

The FireMask product determines whether there is a fire that exists in the pixel at hand. It is based on a two factors, first if there is a sufficient amount of infrared emissions to determine that there is an absolute detection of a fire of sufficient strength. The second factor is whether the detected surface temperature is sufficiently variable as compared to the surrounding pixels' surface temperature approximation, trying to account for variability of the surface temperature and reflection by sunlight.

Furthermore, since the onset of the moonsoon brings sufficiently large amounts of precipitation that it usually leads to the end of the fire season (Cohen, 2014; Hasler et al., 2009), knowledge of the rainfall rate is important. For this, we use TRMM measurements of precipitation, as generated by the 3B42 algorithm. This produces daily average precipitation measurements at 0.25° by 0.25° spatial resolution over the areas of interest for this work.

To validate the results, we also use two additional measurement platforms for AOD from MISR and AERONET. From AERONET (Holben et al., 1998) we either use avaiable AOD at 0.55 µm or interpolate the surrounding measurements to 0.55 µm, at 9 different stations (see Fig. 3) located in the region of interest. We use Level 2.0 data which is cloud screened and validated where a sufficient amount of data is available, and at four stations where it is not, we use Level 1.5 Data. However, in the case where Level 1.5 data is used, we only retain the AOD data when the corresponding Angstrom Exponent is larger than 0.2, giving us reassurance that the product is relatively cloud-free. Although AERONET is the most precise measurement platform, it is limited in spatial coverage. Therefore we also use measurements from MISR (Holben et al., 1998) of AOD at 0.555 µm, with a monthly temporal resolution and a 0.5° by 0.5° spatial resolution.

All of the data used has been taken from from January 2001 through December 2013. In the case of remotely sensed data, it has been aggregated or interpolated

CC BY

respectively to 0.1° by 0.1° spatial resolution and 8-day average temporal resolution, to make it consistent with the LAI measurements. AERONET measurements have also been taken using whatever data was available over the same 8-day periods, and have been considered to be representative of the entire corresponding 0.1° by 0.1° box in which they are located. A summary of the data used in this work is displayed in Table 1.

2.3 Variance maximizing analysis technique

Aerosol emissions and resulting changes in AOD in the Southeastern Asia region mainly comes from two types of sources: urban/anthropogenic and fires. Emissions of aerosols from urban/anthropogenic include those from cities, transportation, and industrial processes, which generally include temporally and geographically regular combustion of coal, oil, and natural gas throughout the year. On the other hand, emissions of aerosols from fires, which include clearing of forests, agriculture, peat, and rubbish, are more highly irregular over space and time, preferentially occurring under certain economic conditions as well as during periods of dryness, due to either changes in irrigation or under the influence of various meteorological/climatological conditions (Cohen, 2014). As the ultimate goal of this study is to develop an understanding and constraint on the absolute source of aerosol emissions, and since fire is the most uncertain contribution in this region, therefore the analytical technique must target the large amount of variance in the measured fields of the AOD. In specific, those regions which both contribute the most to the variance of the AOD field as well as correspond to a large annual amount of absolute are the regions which which are most likely fires. A simple check of the geography can then be done to eliminate any false positives that are known to be urban or industrial regions. Further, observed land-use changes should correspond, and the NDVI and LAI are used for this purpose.

To achieve these goals, we first employ the Empirical Orthogonal Functions/Principal Component Analysis technique (EOF/PCA) on the 8-day average MODIS AOD product. The EOF/PCA analysis provides a decomposition of a given set of data **F** into subcomponents that contribute the most to the overall variability (Björnsson and Vene-

ACPD
15, 26895–26957, 2015

CC BY

gas, 1997). This is done by decomposing the measurements into independent (orthogonal) spatial/geographic modes $\mathbf{S}_i$ and their associated temporal/time modes $\mathbf{T}_i$, as explained in Eqs. 1–5.

$$\mathbf{F} = \begin{pmatrix} a_{11} & \cdots & a_{1M} \\ \vdots & \ddots & \vdots \\ a_{N1} & \cdots & a_{NM} \end{pmatrix} \tag{1}$$

$$\mathbf{F}^T\mathbf{F} = \mathbf{C}\mathbf{Y}^T\mathbf{Y}\mathbf{C}^T \tag{2}$$

$$\mathbf{S}_i = \begin{pmatrix} c_{1i} \\ \vdots \\ c_{Ni} \end{pmatrix} \tag{3}$$

$$\mathbf{T}_i = \begin{pmatrix} y_{1i} \\ \vdots \\ y_{Ni} \end{pmatrix} \tag{4}$$

$$\mathbf{F} = \mathbf{Y}\mathbf{C}^T = \mathbf{T}_1\mathbf{S}_1^T + \cdots + \mathbf{T}_N\mathbf{S}\mathrm{N}^T \tag{5}$$

2.4 Regression-fit model connecting land use change to AOD

Along with the analysis, we also employ a simple multi-variable linear regression model to predict AOD from measured land-use and meteorological variables. This approach is adapted because of the physical nature of the relationship between these variables. Fires lead to a direct drop in LAI in currently growing vegetation through the combustion process. In the case of agriculture which has already been harvested, the LAI would have previously dropped, while the dried products are left to burn. Similarly if there is a change in the vegetation/agricultural state after the fire, this should show up by a restored LAI which is of a different magnitude. NDVI would similarly be impacted,

Discussion Paper | Discussion Paper | Discussion Paper | Discussion Paper |

ACPD

15, 26895–26957, 2015

Estimating AOD from meteorology and land-use over Southeast Asia

J. B. Cohen and E. Lecoeur

CC BY

as the chlorophyll is combusted along with the plant material that is associated with it. Furthermore, if there is a loss of efficiency of the land surface associated with the fires, this should also show up in a long-term change in the NDVI.

Furthermore a lack of precipitation or drier conditions will increase the amount, intensity, and duration of the fire, while an increase in precipitation will either reduce the intensity of the fires or stop them all together. This relationship is slightly more complex, since there are cases where small amounts of precipitation reduce the energy of the fire, but lead to an increase in AOD due to a switch from flaming to smoldering. However, these cases are over and beyond the approach taken here. Yet, in reality the surface wetness, which is some function of LAI, NDVI, and precipitation, is an even more effective measure, and hence we are hoping that the linear-regression format employed here can capture this physical variable, at least to some extent (Fisher et al., 2009; Phillips et al., 2010; Wohl et al., 2012).

To ensure that the impact of fires is physically as expected on AOD, in which an increase in fire should lead to an increase in emissions and hence AOD, we employ two different regression equations. Both equations use LAI, NDVI and Precipitation as predictive variables Equation (7), while only one equation (Eq. 6) also uses FireMask. The regression coefficients α_i, β_i, γ_i, and δ_i are computed that minimize the root-mean-square errors while solving the following equations:

$$\mathrm{AOD_{MODIS}} = \alpha_1 \cdot \mathrm{LAI} + \beta_1 \cdot \mathrm{NDVI} + \gamma_2 \cdot \mathrm{RAIN} + \delta_1 \cdot \mathrm{FireMask} \quad (6)$$

$$\mathrm{AOD_{MODIS}} = \alpha_2 \cdot \mathrm{LAI} + \beta_2 \cdot \mathrm{NDVI} + \gamma_2 \cdot \mathrm{RAIN} \quad (7)$$

Using the constrained values from the equations above, the AOD can be approximated during different seasons or over different areas, such as those which are cloud-covered and hence do not show measurements. These reconstructed values are generated and specifically compared against AOD values from other measurement platforms, specifically MISR and AERONET.

Since the nature of the land-use change, the amount of precipitation, the state of native vegetation, and the strengths and timing of the AOD signal are different over the

ACPD
15, 26895–26957, 2015

two regions, we compute the fitting for AOD over reach region separately. This helps us to aim to better quantify and understand the relationships between these variables when fires occur. This is especially important in southern Southeast Asia, where there is stronger year-to-year variability, the issue of cloud-cover is much more pronounced while coupled with much shorter ground station measurement sites, leading to a situation where data is more constrained to both form and evaluate the fits properly.

To test seperately only the fire-occuring seasons, we define fire activity periods over each region as the daysduring which which $\mathbf{T}_1$ and $\mathbf{T}_2$ respectively are above a certain threshold τ_{North} and τ_{South}. Different thresholds for $\mathbf{T}_1$ and $\mathbf{T}_2$ are tested, based on the percentile P of the time series beneath the point τ if the time series were to be regrouped and sorted. We hence use the points $P = \{0.90, 0.835, 0.75\}$.

3 Results

The subsequent analysis performed using the variance maximizing analytical technique only retains those modes $\mathbf{S}_i$,$\mathbf{T}_i$ that explain at least 5 % of the total variability. This is to ensure that any signal found is larger than the uncertainty in the measurements themselves, and hence should be physically relevant. Using this constraint, there are two modes $i = \{1,2\}$ that explain the variability in the 8-day MODIS AOD measurements (see Fig. 3). 38 % of the variability in the AOD field maps to region $i = 1$ as shown in Fig. 2a, and which we will hence refer to as northern Southeast Asia. 13 % of the variability in the AOD field maps to region $i = 2$ as shown in Fig. 2b, which we will hence refer to as southern Southeast Asia. The physical relevance of these mathematical modes is established by correlating the computed measured average AOD over the respective regions $\mathbf{S}_i$ with the respective Principal Component $\mathbf{T}_i$. When this is done, it is found that there is 86 % correlation over in northern Southeast Asia and 77 % correlation over southern Southeast Asia, as shown in Fig. 2c and d.

Over northern Southeast Asia there is a partially bi-annual peak, with some years having a single peak and others have two peaks. The major peak, which is the more

CC BY

pronounced or sole peak, occurs every year in the measured AOD averaged over $\mathbf{T}_1$ during the latter part of the local dry season (from mid-February to late-April). Looking at the average value of the time series of the AOD measurements over $\mathbf{S}_1$, it is found that the AOD peaks at the same time as $\mathbf{T}_1$ peaks, and that the average AOD ranges from 0.46 to 0.86, depending on the year. The smaller peak occurs in August and September as shown in $\mathbf{T}_1$ in most of the years (but not in 2008, 2010, and 2011). Similarly, the average of the measured AOD over the region $\mathbf{S}_1$ during the same months and years has a corresponding peak ranging from 0.40 to 0.63 during the years when the second peak occurs. The only disagreement between $\mathbf{T}_1$ and the measured time series of averaged AOD over $\mathbf{S}_1$ occurs during 2003, which has already been noted previously by (Cohen, 2014).

Over southern Southeast Asia, there is a one-to-one agreement between the peaks in $\mathbf{T}_2$ and the peaks in the averaged measurements of AOD over $\mathbf{S}_2$, with the peaks occuring in 6 years (2001, 2002, 2004, 2006, 2009, and 2012) and not occuring in the other 7 years. The measured peak in the average AOD ranges from 0.5 to 1.2, indicating that when these events occur, their impact on the aerosol loading is larger than in northern Southeast Asia. The timing of the peaks is also wider and less well constrained than in northern Southeast Asia, corresponding to most of the entire dry season, from early-August to the end of October. Furthermore, there is no observed second or smaller peak.

However, the issue of cloud cover leading to missed positives is observed in southern Southeast Asia. While this method was able to pick up the high haze and pollution years of 2002, 2004, the El-Nino in 2006, and 2009, two additional high haze and pollution years of 2010 and 2013 were not captured. As already shown in (Cohen, 2014), which was capable of capturing 2010 and 2013, the likely cause is cloud cover. We have confirmed that the MODIS cloud cover is in fact the culprit, with there being so few retrievals during these two years that the contribution to the overall variance of the total dataset is reduced, and hence they do not show up under the same spatial pattern $\mathbf{S}_2$, or at a level of energy which can pass the 5.

ACPD
15, 26895–26957, 2015

CC BY

Careful consideration of $\mathbf{T}_1$ (see Fig. 2c) shows that it is considerably more noisy than $\mathbf{T}_2$ (see Fig. 2c), and there are three explanations for this. First is because part of the emissions from the region are more complex. In addition to the fires, there are large urban sources from three megacities: Bangkok, Ho Chi Minh City, Hanoi, as well as many highly populated and inhabited areas outside of these cities throughout the countryside. The emissions from these cities is consistent throughout the year, and therefore the high frequency noise in these emissions, such as day/night differences, weekday/weekend differences, etc. tends to make the signal slightly more noisy. Secondly is that the fires in this region are due to combination of a few factors, which occur on different scales and have various different size holdings in each case, meaning that small differences in timing, intensity, and duration are to be expected from when the people decide to burn and how long they decide to burn for (Taylor, 2010). There is agricultural/straw burning in Thailand, subsistence burning in Cambodia, forest clearing in Myanmar and Laos, and urban and agricultural expansion in Vietnam, with some of these agricultural regions, especially related to rice, having 2 crops a year, and hence the possibility of being burned more than once (Dennis, 2005; Tipayarom and Oanh, 2007). Thirdly, the dry season here tends to be extremely dry, without even occasional rainstorms. Therefore, any emitted particles tend to have a very long lifetime. Hence, the impact of secondary chemistry is important. This chemistry tends to be very sensitive to the emissions ratios, to clouds, and to any non-linearly emitted secondary species from urban areas as the plums proceeds downwind. On the other hand, in southern Southeast Asia, the population is also large, but in many of the places in Indonesia and Malaysia that are source regions, the cities are large and well contained, while the countryside is still relatively empty. Secondly, in this region, the major cause of burning is the clearing of primary forests, and much of this is done by a smaller number of large-land holders, further reducing the variability. This is especially so on a year-to-year basis, during some years which there is relatively little burning at all. Finally, even during the dry season, there is still a considerable amount of small scale convective precipitation and day/night sea/land breezes and rain. Hence, the lifetime of

ACPD
15, 26895–26957, 2015

CC BY

the particles and secondary precursors tends to be slightly shorter, and the impacts of non-linear secondary processing is also reduced. Hence, the fact that southern Southeast Asia often has an even higher average AOD, means that the emissions must be considerably larger in terms of magnitude from year to year, although not necessarily more variable within each year, as also found in Cohen (2014).

These results are clearly consistent with the time-averaged values of the land-use measurements of LAI and NDVI when averaged over regions $\mathbf{S}_1$ and $\mathbf{S}_2$ respectively. Over $\mathbf{S}_1$, we can clearly see that much of the region either has an average LAI which is far too low to correspond to native of secondary forest, implying that the land is now agriculture. In other cases, there is still a high average LAI value with a corresponding reduction in NDVI, implying that primary forest is being deforested in exchange for some type of commercial agricultural tree crop, such as palm oil, rubber, or wood for paper. However, the region over which this second category is occurring is smaller in size than the first region with the simultaneous decrease in both LAI and NDVI (Huete et al., 2002; Myneni et al., 2002, 2007). On the other hand, over the region $\mathbf{S}_2$ we find that the LAI is still generally quite high throughout the region of interest, while the average NDVI is falling at an even faster rate than the drop over the smaller region in $\mathbf{S}_1$ in which a similar type of condition is occurring. This is completely consistent with the known large-scale deforestation occurring throughout Indonesia and Malaysia where mostly primary forest is burned and replaced with large-scale agricultural tree-based crops (Dennis, 2005; Phillips et al., 2010; Taylor, 2010; Wooster et al., 2012; Field et al., 2009).

A spatial mapping of the climatological mean and standard deviations of LAI and NDVI over Southeastern Asia are displayed in Fig. 1. First, it is observed that the LAI is smaller in average over northern Southeast Asia (LAI = 2.3) then over southern Southeast Asia (LAI = 3.5). Similarly for NDVI, the average value over northern Southeast Asia is (NDVI = 0.61) while it over southern Southeast Asia it is (NDVI = 0.70). This is consistent with the knowledge that in northern Southeast Asia, the land has been more altered from its base tropical rainforest state (Hasler et al., 2009; Taylor, 2010). In

ACPD
15, 26895–26957, 2015

CC BY

fact, there is a considerable amount of rice and other agriculture which has completely replaced trees with crops. Also, the pace of forest clearing is quite rapid in those regions which still retain a considerable amount of native forest. The only considerably widespread regions of native forests remain in Laos and and at the frontier regions near the intersection of Laos, Thailand, and Myanmar.

3.1 Influence of measured fires

To look at the impacts of measured fires from MODIS, we fit the relationships between LAI, NDVI, Precipitation and AOD in two cases, both with and without the inclusion of the FireMask variable using Eqs. (6) and (7). This is done seperately over both the northern and southern regions with the corresponding different thresholds. A comparison of the time series of the region averaged AOD from each EOF region, the 4 model predicted AOD values, and the MODIS averaged AOD is made. The average statistical error and average statistical correlation between the datasets and the regression–fit model predicted AOD used to determine which threshold τ is ultimately used for the purpose of determining the best fit coefficients for α, β, γ, and δ. The resulting statistics are displayed in Table 2.

As expected, including the FireMask variable significantly increases the performance of the algorithm in terms of correlations: on average the correlation increases from 70 to 79 % in the northern region, and from 66 to 75 % in the southern region. However, there is no improvement in the mean error between the reconstructed data and the original measured AOD. This means that the existence of fire offers an improvement in determining the spatial and temporal timing of the fires, but does not help to estimate the intensity of the AOD or hence the emissions. This is physically consistent, since the actual emissions should be a more complex function of the type of burning, the material burned, and the conditions under it was burned, not just the existence of a fire. Additionally, this is consistent because the FireMask product only quantifies the likelihood of a fire occuring within the given pixel, but provides no information on the intensity of the fire. Furthermore, the results of the fitting of the regression coefficient

CC BY

associated to FireMask (Fig. 4) show that the coefficient is strongly positive over the regions where fire are the most important and AOD variability the strongest (regions within the dots). Thus, the results are found to be consistent with what is understood, that FireMask is a reasonable predictor of emissions of aerosols from fires, but that this factor is only useful as a predictor of the effect, not as a means of understanding the magnitude of the effect.

The best fit regression coefficients associated with NDVI make more physical sense in the case where the FireMask predictor is used Eq. (6) (Fig. A2a) than in the case where it is not Eq. (7) (Fig. A2b). In general a negative coefficient is found, which implies that regions will lose NDVI as a result of an increase in AOD, which is consistent with the health of the land decreasing during a fire. A similar gain is also found in terms of the best fit coefficients for LAI in the regions which are not rice dominant (rice has a significantly low LAI so that the signal to noise ratio from the satellite product is too low to produce a statistically significant result over these regions). The regression coefficients are thus consistent and for this reason, we only refer to Eq. (6) from this point forward.

Making comparisons between the regression constructed AOD and the measured AOD from MODIS AOD_{MODIS} over northern Southeast Asia leads to the determination that in average, using τ_{North} = P75(PC1) as the threshold of fire activity leads to the best results, as shown in Table 2. This leads to the reasonable conclusion that in order to represent the AOD during the fire season well, there must be greater access to data, while to represent the AOD during the non-burning or low-burning seasons, that less data is required. This is consistent with the variability being considerably larger during the burning season in both space and time over the region of interest.

On the other hand, for southern Southeast Asia, using a very small value of τ_{South} = P12.5(PC2) gives the best statistics. This means that using less data improves the fit during the fire season as compared to the use of more data which better constrains the fit over the whole year. This is not intuitive and is only consistent with the case that either (a) the data is more likely to be of low quality during the burning season (i.e. the

ACPD
15, 26895–26957, 2015

J. B. Cohen and E. Lecoeur

Title Page
Abstract Introduction
Conclusions References
Tables Figures
◀| |▶
◀ ▶
Back Close
Full Screen / Esc
Printer-friendly Version
Interactive Discussion

CC BY

data is corrupted by clouds), or that there is a considerable amount of data missing during the burning season (which is also possible due to the widespread distribution of clouds over much of both Borneo and Sumatra). This view is also consistent with the year-to-year and decadal scale of variability, wherein some years will have little to no fire, and hence data is required over a considerably longer period of time, including both high- and low-fire years in order to properly reproduce the observed patterns. For the remaining of this analysis, we only consider (1) that the reconstructed data set of AOD over the northern region has been computed by using τ_{North} = P75(PC1) as fire threshold, and (2) that the reconstructed data set of AOD over the southern region has been computed by using τ_{South} = P12.5(PC2) as fire threshold. These two data sets will be referred as AOD_{REC}^{North} and AOD_{REC}^{South}.

3.2 Comparing AERONET measurements over northern Southeast Asia

Seven stations from AERONET are situated within the northern region (Chiang Mai, Pimai, Bac Giang, Nghia Do, Vientiane, Mukdahan, and Ubon Ratchathani) and four stations are located inside the southern region (Jambi, Kuching, Palangkaraya, and Singapore). The location of those stations is displayed in Fig. 3 and complementary information is available in Table 3. Of these stations, three are urban sites located downwind from burning regions: Singapore, Bac Giang and Nghia Do, while the remaining sites are located directly in or adjacent to burning areas.

Figures 5 and 6 display the temporal series of the AERONET AOD (black curve) and regression–fit modeled AOD (blue curve) at the seven stations situated within the northern region. Tables 6 and 7 displaying the statistics of the goodness of fit between the MODIS measured AOD and the reconstructed AOD respectively, AOD_{MODIS} and AOD_{REC}^{North}, in terms of reproducing the AERONET measured AOD signal. These statistics are computed over both the entire time series that the respective AERONET station is measuring (Table 6) and well as only during high pollution episodes. The first general observation is that all AERONET stations in northern Southeast Asia have an annual

ACPD
15, 26895–26957, 2015

CC BY

peak in their AOD which occurs during the fire season, with this peak occurring from February through April each year. Additionally, each station has a smaller second peak over many of the years, but not annually, occurring sometime in August or September.

There are two remote stations, which are in regions which are neither urban nor in the process of urbanizing: Pimai (Fig. 5c) and Ubon Ratchathani (Fig. 5d). At both stations, AOD reaches its maximum value of over 0.5 during the fire season, while generally the values are considerably clean throughout the rest of the year, as shown in Fig. 5c and d. At these stations, the high AOD events occur every year in February to April and a second local maximum occurs from September to October in roughly half of the years: 2001 to 2006, and 2009, with the second local maximum AOD peak being of around 0.46. At Pimai, the AERONET data shows high pollution during the fire season every year from 2003 to 2008. The model captures all these events correctly in terms of duration, with the onset and end times slightly off, leading to a correlation of 43 %. However, the intensity (mean error of −0.12) (see Table 7). At Ubon Ratchathani, the AERONET data shows high pollution events during the fire season of the years 2010 to 2012. The model captures all these events in terms of duration (correlation of 80 %) but also underestimates its intensity (mean error of −0.22) (see Table 7). A large peak of high AOD can been seen on the AERONET data at Ubon Ratchathani in September 2012 corresponding to a high-pollution event in Singapore (see Fig. 7d). This peak, which has a maximum AOD value of 0.6, is captured by the model. During the common years of data between AERONET and $\text{AOD}_{\text{REC}}^{\text{North}}$ (2008 to 2013), we can see that the model captures the fire season and the pollution that is generated by it well, both in terms of duration (correlation is 64 %, but not in terms of intensity (mean error of −0.26) (see Table 7).

There are three stations which are situated at medium-sized urban sites which are also adjacent to or directly upwind from fire burning regions: Chiang Mai, (Fig. 6a), Mukdahan (Fig. 6b), and Vientiane (Fig. 6c). It is shown that there is a strong annual peak during the fire season from February to April at these stations. At Chiang Mai and Mukdahan, which are both nearer the up-wind regions where the agricultural

ACPD
15, 26895–26957, 2015

CC BY

fires occur, the maximum value for AOD is around 0.5, while it is around 0.6 at Vientiane, which is located near the downwind edge of the agricultural burning regions. Figures 6a–c also show smaller peaks during other parts of the year: from September to October for the years 2001 to 2006 at Chiang Mai, with a maximum AOD value of 0.4; from July/August and to October/November (depending on the years) for the years 2001 to 2007, 2009, and 2010 at Mukdahan, with a maximum AOD value of 0.44; and from September to October for the years 2001 to 2007, and 2009 at Vientiane, with a maximum AOD value of 0.59. The nature of these secondary peaks are not annual in occurrence, and an explanation will be explored in more detail later on. At Mukdahan, the AERONET data demonstrates the fire season peak for every year the data exists: 2004, 2006, 2007, 2008, and 2009. The regression–fit model reproduces the high pollution every year ($R^2 = 0.69$), while also reproducing the intensity correctly in 2007 and 2009. While there is only very sparse AERONET data at Vientiane, the regression–fit model reproduces the signal well ($R^2 = 0.64$ and RMS = −0.07) (see Table 6). Finally, the model also captures the high pollution events measured in March, April, and September 2012.

As expected, there is a considerable amount of variability at stations which are in or near large urban areas (Megacities), due to the combination of both the fire signal as well as local emissions and in-situ secondary processing, as shown in Table 4. In particular, the signals at the two stations near to the rapidly growing urban megacity of Hanoi, the capital of Vietnam, Bac Giang (Fig. 5a) and Nghia Do (Fig. 5b) are very similar. These stations have a much higher annual average AOD than the other stations in the region, with the daily average value as well as long-term mean measured AOD being frequently in the polluted range (AOD larger than 0.4), and the annual high AOD peak having a yearly maximum of at least 0.9 at both of these stations (see Table 5). Figure 5a and b also show smaller AOD peaks (maximum value of around 0.7) during other parts of the year (from July through November depending on the year). During the fire seasons in 2004 and 2007 at Bac Giang, the timing of the high pollution events

ACPD
15, 26895–26957, 2015

CC BY

are well-captured by the regression–fit model, in terms of onset, duration, and end time, although the model intensity is underestimated.

In 2006, the southern Southeast Asian fire season produced an extensive and massive amount of emissions $\mathbf{T}_2$ due to extremely dry and warm conditions brought on by the El-Nino conditions. Various models and measurements have shown that the fires from these emissions have spread from $\mathbf{S}_2$ throughout the Indian and Pacific Oceans (Podgorny et al., 2003). However, we have also found that the signal is clearly present at all of the stations located in $\mathbf{S}_1$, in terms of AERONET measurements as well as regression–fit models. At Chiang Mai, Mukdahan, and Pimai both the intensity of the 2006 season as well as its onset, duration, and conclusion are all well reproduced in both the AERONET measurements and the regression–fit model. Even at the urban megacities Bac Giang and Nghia Do the AERONET measurements also display a high pollution peak (AOD = 1.2) around September 2006, while the regression models at both of these stations capture the measured onset, duration, and ending of this event. The only issue is that the magnitude of the regression–fit model AOD underestimates the measured value by as much as 33 % at Bac Giang. Unfortunately the other AERONET stations do not have measurements available during this event.

Given the intimate connection between fires and the ensuing rapid changes of the land surface which occur at the same time, we now explore how the LAI and NDVI have changed at the same locations as the AERONET stations. First, they show a correspondingly higher value in both of these variables during the second, localized peak, than at the major annual peak, with a maximum value of around 0.9 at these stations (see Table 5). Figure 5a and b also show smaller AOD peaks (maximum value of around 0.7) during other parts of the year (July through November depending on the year), see Tables 3 and 5. This is indicative that the second peak, which does not occur year-to-year, may not be attributed to large-scale local burning, unless either the local fires are much less extensive, and thus do not lead to significant change in the land surface, but happen to just be upwind of these measurement stations in these given years, or that the local fires are much more polluting per unit of land use change, and

ACPD
15, 26895–26957, 2015

CC BY

hence still contribute to the AOD to some extent. The other possible explanations are that the pollution during these times is actually transported from other place, or are intensified due to some sort of secondary processing. However, it is also found that these changes in the year-to-year LAI and NDVI values do not vary in a one-to-one manner with $\mathbf{T}_2$, which has some covariance during the big fire years of 2002, 2004, 2006, and 2009, but not during other years in which the peak occurs, such as 2001, 2003, 2005, and 2007.

Hence, we are able to conclude that the annual peak in AOD as measured at these AERONET stations throughout $\mathbf{S}_1$ has an annual peak which is clearly due to fires, and that this is true for both urban, partially urban, and remote sites. Further, during these fire events, the dominant source contributing to the peak in AOD is from the burning itself, even in the urban areas. Additionally, there is a second peak found at these stations, which is both smaller in magnitude, and only occurs in certain years. This secondary peak is very likely not due to local burning, and instead it is shown that a significant number of these years co-vary with analyzed large-scale fires from region $\mathbf{S}_2$. However, since there are a few years during which this is also not the case, it is possible that other sources of long-range transport or secondary production of aerosols, such as from South Asia, could also contribute.

3.3 Comparing AERONET measurements over southern Southeast Asia

In southern Southeast Asia, $\mathbf{S}_2$, the majority of the emissions come from a small number of well-defined major urban centers, transport lines through the waterways, and wide-spread sources from fires, with much of the region still continuing primary forest or dense secondary forest. As a consequence, the major source of the variation in the AOD is a combination of the emissions from fires and precipitation (as it is the major source of the aerosols removal from the atmosphere). This is demonstrated in Fig. 7, demonstrating a smoother and less variable set of measurements during the wet season than at sites over northern Southeast Asia, Figs. 5 and 6. Consequently,

ACPD
15, 26895–26957, 2015

CC BY

the AERONET site in Singapore, the sole large urban area in $\mathbf{S}_2$, is very different from the other stations of this subregion.

Unlike in northern Southeast Asia, in general, the AOD signal in southern Southeast Asia tends to only peak once a year (except for in 2009 and 2014, which are special cases to be discussed later that had 2 peaks due to primary fire emissions). This primary peak, as shown in $\mathbf{T}_2$ always occurs during the local fire season from August through October/November, without any additional second peak occurring during a non-burning period, as in $\mathbf{T}_1$. Effectively, this implies that emissions from $\mathbf{S}_1$ are not contributing to the variance in the measured AOD over $\mathbf{S}_2$ and that long-range transport from northern Southeast Asia is not efficient in contributing to the high peaks in AOD found over $\mathbf{S}_2$.

Additionally, southern Southeast Asia has an important source of uncertainty and bias in the measurements over the region. Specifically, the impact of intense cloud cover is also determined to be very important, in terms of being able to capture all of the known large-scale fire based events. We observe that in a few special cases where known large-scale pollution events have occurred over $\mathbf{S}_2$ as measured both on the ground and by MISR measurements of AOD (Cohen, 2014), that MODIS was not able to successfully capture the events (for example: June 2013). A careful examination of the cloud cover fields from MODIS and the FireMask measurements show that this is clearly the case, at least for June 2013; the region $\mathbf{S}_2$ was almost completely masked by clouds (over 80 % of all pixels) in the day-to-day tracks, with more than 90 % of pixels in the 8-day average fields over this period of time being masked.

The AERONET station in Singapore is located in a highly urban environment, with sizable sources of aerosol emissions related to shipping, a high energy using population, and refineries. It is clear that there are no wild-fires occurring within Singapore. At the Singapore station, we observe an annual signal except for every year, although during the years 2008 and 2010, the signal is less intense than in the other measured years. There is a considerable amount of variation in the magnitude, the onset, and the duration of the peak, as well as a considerable amount of noise. However, the maxi-

ACPD
15, 26895–26957, 2015

CC BY

mum measured AOD here on an 8-day average basis, ranges from a low year of 0.55 to a high year of 0.81 in 2006. Even though the fires were quite distant, it is clearly observed that then most intense event in 2006 is readily captured here, further supporting that even in an urban environment, Singapore offers a reasonable downwind signal site for observing the impacts of the fires.

On the other hand, the other AERONET stations in this region, including in Kuching, Jambi, and Palangkaraya, are situated in remote and mostly heavily jungle/forested regions of Borneo and Sumatra islands (see Table 3). These sights are all located close-by to where the fire sources originate, in the jungles and forests of Borneo and Sumatra. The AERONET station in Jambi, situated on Sumatra Island, has an annual signal of high AOD occurring once a year, every year, except in 2010 (where there were no corresponding measurements during the peak season) (see Table 9). However, the magnitude, onset, and duration of these high pollution events is highly variable from year to year. The AOD maximum value ranges from a low of 0.67 (in 2007) to a high of 1.49 (in 2006) (see Table 8). The AERONET station in Kuching, situated Northern Borneo, in Malaysia, also has an annual peak signal in AOD every year that measurements are available (there were no measurements during the corresponding peak times in 2008, 2010, and 2013). The magnitude, start, and duration of this peak is again highly variable from year to year, with the maximum in measured AOD ranging from a low of 0.68 in 2007 to a maximum of 1.36 in 2006. At Palangkaraya, which is situated in western Borneo in Indonesia, there is also a single high peak occurring every year, except for 2010 (which again did not have any measurements during the high fire season). Similar to the other stations, the intensity, onset, and duration of the high AOD signal was very variable from year to year.

The regressive-fit model based on the MODIS measurements at each of the remote sites in southern Southeast Asia: Jambi, Kuching, and Palangkaraya, is capable of reproducing the major heavily polluted years as found in the measurements, including 2002 (max AOD of 1.24 in Jambi, 1.0 in Kuching, and 1.94 in Palangkaraya), 2004 (max AOD of 0.99 in Jambi, 0.85 in Kuching, and 1.18 in Palangkaraya), 2006 (max AOD of

ACPD
15, 26895–26957, 2015

cc BY

1.49 in Jambi, 1.4 in Kuching, and 1.98 in Palangkaraya), and 2009 (max AOD of 0.95 in Jambi, 0.87 in Kuching, and 1.02 in Palangkaraya). At Jambi and Palangkaraya, the regressive-fit model reproduces the high AOD event of late 2012 well, with a better correlation with the AERONET measurements ($R^2 = 76\,\%$ at Jambi and $R^2 = 74\,\%$ at Palangkaraya) the the actual MODIS AOD at the same grid point ($R^2 = 51\,\%$ at Jambi and $R^2 = 71\,\%$ at Palangkaraya), as given in Table 10, although the intensity in these years is slightly low. On the other hand, the regressive-fit model reproduces the AOD well in terms of intensity, onset, and duration at Kuching (RMS error of 0.13, $R^2 = 66\,\%$) (see Table 10). However, the regressive-fit model is still basically constrained by the cloud cover issue. It is for this reason that the know high values of aerosols in the atmosphere over Singapore in June of 2013 (as based on surface measurements and personal observation) is not captured in AERONET measurements, MODIS measurements, or the regressive-fit model. In addition to June 2013, we also find that MODIS AOD and the regressive fit model are both not capable of capturing the 2010 fire season peak either. However, the issues of cloud cover seem to be less important in other years, and we find the onset, duration, and intensity are all well matched between the regressive-fit model and AERONET measurements at Singapore during the fire seasons of the years 2007, 2008, 2009, 2011, and 2012 (see also Tables 10 and 11 for statistics).

3.4 Comparisons vs. measurements from the MISR satellite

MISR satellite measurements of AOD are at lower spatial and temporal resolution than MODIS and AERONET measurements, and thus to use them as a basis for comparison, the values from MODIS and AERONET will be averaged to a monthly-basis as well as at $0.5^\circ \times 0.5^\circ$. Over northern Southeast Asia, the time series of the regression–fit model AOD compares very well with the time series of the average MISR AOD over the same region ($R^2 = 0.77$ over all of $\mathbf{S}_1$, and $R^2 = 0.85$ over the region of highest variability). While there is some underestimation of the absolute AOD as compared to the MISR measurements, that underestimation is always less than 0.1, and therefore is

ACPD
15, 26895–26957, 2015

J. B. Cohen and E. Lecoeur

CC BY

not far from the order of magnitude of the error in the measurements themselves. One of the important reasons why the agreement is so good is that this region is generally cloud-free during the dry season when the fires occur, and hence there is a quite large and representatively similar sampling size between MODIS, MISR, and AERONET during the fire periods in this region. This establishes that indeed the MODIS based regression–fit model matches well against MISR, and is able to reproduce the variability and magnitude of the AOD over northern Southeast Asia.

Not surprisingly, when fitting the results of the MODIS regression–fit model using 8-day average data, the overall fits are less good when comparing against MISR. Part of the issue is the additional variability, but more importantly is the lack of sufficient data due to cloud coverage. Specifically, over the region $\mathbf{S}_1$, the correlation rises from $R^2 = 0.66$ to $R^2 = 0.81$ when increasing from 8-day to monthly averaging. Similarly, the comparison between the AERONET data and MISR AOD also increases from $R^2 = 0.59$ to $R^2 = 0.79$ when comparing 8-day averages and monthly averages respectively. Overall, the regression–fit model is able to reproduce the variation of AOD at all the stations in northern Southeast Asia, both in terms of duration and intensity concerning high pollution events (see Figs. B1 and B2).

As expected, the spatial comparison between MISR and the regression–fit model over southern Southeast Asia is less good. The first thing to note is that the spatial extent of the region from MODIS, given with the relatively level of high certainty by $\mathbf{S}_2$, is considerably smaller than a similar spatial distribution of the smoke extent over this same region, when analyzed in the same way using data from MISR measurements (Cohen, 2014). This is explained in part due to the larger cloud-covered fraction in the MODIS measurements when compared with MISR, as well as the shorter averaging period with the MODIS measurements, leading to a situation where there is insufficient information at each averaging time step over much of the region. It is found that the RMS error between MISR and the regression–fit model ranges from a minor and relatively insignificant (as compared to the measurement errors) model overestimate of 0.1 in AOD, to a substantial and significant model underestimate in the AOD of up to

ACPD
15, 26895–26957, 2015

CC BY

0.5. This regression–fit model underestimates as compared to MISR measurements is significantly larger than the AERONET and MISR disagreement over this region, which is less than 0.3 (Cohen, 2014; Shi et al., 2011) and further, this error occurs especially and exclusively during the intense fire-burning years. On the other hand, the overall temporal correlation between the regression–fit model and the time-average AOD from MISR is $R^2 = 0.72$ over all and is as high as $R^2 = 0.79$ over the region of highest AOD variability. This means that the inter-annual and intra-annual variation is relatively captured by the MODIS measurements and the resulting regression–fit model.

4 Conclusions

An in-depth analysis of multiple measurements from MODIS, MISR, TRMM, and AERONET measurements has been performed over a 13-year period over Southeast Asia. Using MODIS AOD, the spatial and temporal patterns of the contribution of fires to the atmospheric loading of aerosols was established. Two distinct regions, with vastly different properties were observed: one in northern Southeast Asia, which had a strong annual signal with some inter-annual variability, and another in southern Southeast Asia, which had a strong signal with inter-annual and intra-annual variability. Northern Southeast Asia shows an annual high AOD during the fire season (varying roughly from February through April), with a smaller nearly annual peak occurring during the exact timing when southern Southeast Asia has its fire season. Southern Southeast Asia is affected every year by their own fires (from roughly August through October), without any observed secondary peak except for during two exceptionally dry years during the second very short dry season in February 2009 and February 2014. The representation in terms of the timing of the fires of northern Southeast Asia was consistently good in terms of start time, length of the burning season, cessation of the burning, when compared against AERONET and MISR measurements. The representation in terms of timing over southern Southeast Asia was not as good, but still quite acceptable when compared against AERONET and MISR measurements, with the duration

ACPD
15, 26895–26957, 2015

CC BY

of the fire season well captured in strong fire years, and the strongest part of the fire season captured in low fire years.

Bringing in different simultaneous measurements of land-surface variables, and fires from MODIS, and AOD from MISR and AERONET allows us to confirm that these patterns exist and are consistent with land-use burning. Given the difference in the timing and durations of the major monsoon seasons over these regions, the results are consistent. From this point, a simple regression–fit model was established to predict the AOD from measurements of land-use change variables, fires, and precipitation, which should be the basis upon which fires start in the environment. These simple regression–fit models (based on MODIS and TRMM) reproduced the onset, duration, and magnitude of the measured AOD from other sources (MISR and AERONET) well over Southeast Asia. The results of this regression–fit model demonstrate the ability to predict the AOD as observed by AERONET and MISR, using only measurements of land-use change variables and fires from MODIS, and precipitation from TRMM. which should be the basis upon which fires start in the environment.

These simple regression–fit models reproduced the onset, duration, cessation, and even the magnitude of the measured AOD from AERONET and MISR very well in northern Southeast Asia. These simple regression–fit models also reproduced the onset, duration, and cessation, of the measured AOD from AERONET and MISR well well in southern Southeast Asia, especially during the more intense burning years. The main issue in southern Southeast Asia, however, was that the magnitude over this region was strongly underestimated. Some reasons for this include emissions sources which are more variable in space and time, such as the clearing of primary forests, peat burning, and rapid development; and other limiting reasons such as increased cloud cover reducing the number of available measurements over large portions of this region by a significant amount. Further, the inter-seasonal periods in southern Southeast Asia tend to be both more rainy and more cloud-covered than in northern Southeast Asia, due to large scale convection and other regional disturbances like the MJO and the IOD.

ACPD
15, 26895–26957, 2015

CC BY

There is a strong and consistent change in the land use variables occurring during the local fire season over both northern and southern Southeast Asia, although these relationships, as expected, are different over the two regions due to different types of land-use change. The relationships between burning of primary forests, grasslands or crops, and peat should all be different. Additionally, there is an important secondary use for these relationships, determining whether the observed smoke is locally produced of transported from far upwind. For example, it is clearly noted that the land-use changes are much smaller during the second non-annually occurring peak in northern Southeast Asia, implying that while there may be some contribution from local sources, that there is also a large amount of smoke which is transported from other regions. This comes from the idea that if the land itself did not change very much, then the emissions of smoke produced must have been considerably lower. The timing of this smaller peak matches the timing of the fire occurrence over southern Southeast Asia with a very high level of correlation. Additionally, it also cannot be ruled out that the smoke could be urban pollution from South Asia. On the other hand, there is no evidence that any of the smoke in southern Southeast Asia originates from any region other than its own sources.

Further, we explored the added value of using higher temporal resolution data, which is usually thought to add improved value. Due to the large amount of cloudiness encountered, there was a much reduced number of measurements available over southern Southeast Asia during the fire season using 1-day average values as compared to 8-day average values, leading to less statistical relevance. In the end, it was not possible to have a reasonable reproduction of the measured AERONET and MISR values of the onset, duration, and ending of the fires using 1-day average MODIS and TRMM data as compared to when using 8-day average MODIS and TRMM measurements to develop the regression–fit relationships. Even with the 8-day average data and the associated regression–fit relationships, the magnitude of AOD during southern Southeast Asia's fire season is significantly too low, although in northern Southeast Asia, it is low but not more than the magnitude of the uncertainty of the input measurements

ACPD
15, 26895–26957, 2015

cc BY

themselves. The correlation between the regression–fit model AOD and AERONET stations over the entire decadal time period, using 8-day average MODIS data, ranges from $R^2 = 0.42$ to $R^2 = 0.75$. While monthly-average data from MODIS does not provide as fine resolution for the duration, onset, and end times of the fires, it provides the best match in terms of the magnitude of the AOD measurements from AERONET and MISR. However, when using MODIS data on a monthly average basis, the regression–fit model AOD gives a better performance with the correlation coefficient between AOD and AERONET stations ranging from $R^2 = 0.70$ to $R^2 = 0.90$. Furthermore, the correlation over the regions of interest $\mathbf{S}_1$ and $\mathbf{S}_2$ between the regression–fit model and MISR measurements of AOD ranges from $R^2 = 0.57$ to $R^2 = 0.81$. This is due partially to less under-representation of very high short-term peaks, as well as additional data points being available in the MODIS fire and land use products at longer average time durations. This is a counter-intuitive result, with many in the community stressing the added value of higher frequency measurements, but one which is consistent with the fact that such space-born measurements are severely limited by clouds over this region of the world during the fire season. MISR represents the magnitude of the AOD well, with the measurements from monthly-average MISR measurements and monthly-average AERONET measurements being basically the same. Therefore, the ability of the regression–fit model to capture the monthly-average AOD from both MISR and AERONET, in terms of both the inter-annual and intra-annual variability in the fire seasons, is significant, and shows that indeed the changes in the land surface and the impacts of precipitation are what are driving the atmospheric loading of AOD and hence the impact of the fires over this region on the decadal scale. Further, as it is widely known, peat can burn and smolder for am extended period of time after any measured fire has gone away, and therefore, by extending the average value for the fire, it allows for a better matching with the total emissions, which will continue to often be produced for weeks after any visible flame or surface heat is observed.

This study highlights the importance of taking into account land-use variable and precipitation for estimating AOD correctly both in time and magnitude, even if magni-

ACPD
15, 26895–26957, 2015

J. B. Cohen and E. Lecoeur

CC BY

tude remains hard to capture on a 8-day basis. Therefore, the significant bias in the magnitude of the results, must be due to problems of either the relationships over the region being not properly captured, and hence the driving forces of the land-clearing being significantly different than over northern Southeast Asia, or that there is significantly more fire and or land-use change that is occurring in cloud-covered regions, which is not being detected, or some combination of the two (Giglio et al., 2003). This supports the efficacy of the approach introduced here: that it is appropriate to use measured changes in the land, precipitation, and active fires from MODIS and TRMM to reproduce a working model of the atmospheric aerosol loading.

Acknowledgements. This work was supported by the Singapore MOE's AcRF Tier 1 Grant (R-302-000-062-133), the Singapore National Research Foundation (NRF) through a grant to the Center for Environmental Sensing and Monitoring (CENSAM) of the Singapore-MIT Alliance for Research and Technology (SMART), and the Tropical Marine Sciences Institute. The authors also want to thank all of the Principal Investigators of MISR, AERONET, NOAA, MODIS, and TRMM for making the data available.

References

Afroz, R., Hassan, M. N., and Ibrahim, N. A.: Review of air pollution and health impacts in Malaysia, Environ. Res., 92, 71–77, 2003. 26898

Aldrian, E., Gates, L. D., and Widodo, F.: Seasonal variability of Indonesian rainfall in ECHAM4 simulations and in the reanalyses: the role of ENSO, Theor. Appl. Climatol., 87, 41–59, 2007. 26898

Asner, G. P., Scurlock, J. M., and Hicke, J. A.: Global synthesis of leaf area index observations: implications for ecological and remote sensing studies, Global Ecol. Biogeogr., 12, 191–205, 2003. 26901

Björnsson, H., and Venegas, S.: A Manual for EOF and SVD Analyses of Climate Data, Technical Report, Department of Atmospheric and Oceanic Sciences and Centre for Climate and Global Change Research, McGill University, 1997. 26903

Chang, C., Wang, Z., McBride, J., and Liu, C.-H.: Annual cycle of Southeast Asia–Maritime Continent rainfall and the asymmetric monsoon transition, J. Climate, 18, 287–301, 2005. 26898

Cohen, J. B.: Quantifying the occurrence and magnitude of the Southeast Asian fire climatology, Environ. Res. Lett., 9, 114018, doi:10.1088/1748-9326/9/11/114018, 2014. 26897, 26898, 26899, 26901, 26902, 26903, 26907, 26909, 26917, 26920, 26921

Cohen, J. B. and Prinn, R. G.: Development of a fast, urban chemistry metamodel for inclusion in global models, Atmos. Chem. Phys., 11, 7629–7656, doi:10.5194/acp-11-7629-2011, 2011. 26897

Cohen, J. B. and Wang, C.: Estimating global black carbon emissions using a top-down Kalman Filter approach, J. Geophys. Res.-Atmos., 119, 307–323, 2014. 26897, 26899, 26901

Cohen, J. B., Prinn, R. G., and Wang, C.: The impact of detailed urban-scale processing on the composition, distribution, and radiative forcing of anthropogenic aerosols, Geophys. Res. Lett., 38, L10808, doi:10.1029/2011GL047417, 2011. 26898

Dennis, Rona A., Mayer, J., Applegate, G., Chokkalingam, U., Pierce Colfer, C. J., Kurniawan, I., Lachowski, H., Maus, P. Pandu, Permana, R., Ruchiat, Y., Stolle, F, Suyanto, and Tomich, T. P.: Fire, people and pixels: linking social science and remote sensing to understand underlying causes and impacts of fires in Indonesia, Hum. Ecol., 33, 465–504, doi:10.1007/s10745-005-5156-z, 2005. 26897, 26908, 26909

Dubovik, O., Smirnov, A., Holben, B., King, M., Kaufman, Y., Eck, T., and Slutsker, I.: Accuracy assessments of aerosol optical properties retrieved from Aerosol Robotic Network (AERONET) Sun and sky radiance measurements, J. Geophys. Res.-Atmos., 105, 9791–9806, 2000. 26898

Field, R. D., van der Werf, G. R., and Shen, S. S.: Human amplification of drought-induced biomass burning in Indonesia since 1960, Nat. Geosci., 2, 185–188, 2009. 26897, 26909

Fisher, J. B., Malhi, Y., Bonal, D., Da Rocha, H. R., De Araujo, A. C., Gamo, M., Goulden, M. L., Hirano, T., Huete, A. R., Kondo, H., Kumagai, T., loescher, H. W., Miller, S., Nobre, A. D., Nouvellon, Y., Oberbauer, S. F., Panuthai, S., Roupsard, O., Saleska, S., Tanaka, K., Tanaka, N., Tu, K. P., and Von Randow, C.: The land–atmosphere water flux in the tropics, Glob. Change Biol., 15, 2694–2714, 2009. 26905

Fuller, D. and Murphy, K.: The Enso-fire dynamic in insular Southeast Asia, Climatic Change, 74, 435–455, doi:10.1007/s10584-006-0432-5, 2006. 26897

ACPD
15, 26895–26957, 2015

Estimating AOD from meteorology and land-use over Southeast Asia

J. B. Cohen and E. Lecoeur

CC BY

Giglio, L., Descloitres, J., Justice, C. O., and Kaufman, Y. J.: An enhanced contextual fire detection algorithm for MODIS, Remote Sens. Environ., 87, 273–282, 2003. 26899, 26901, 26925

Giglio, L., Csiszar, I., and Justice, C. O.: Global distribution and seasonality of active fires as observed with the Terra and Aqua Moderate Resolution Imaging Spectroradiometer (MODIS) sensors, J. Geophys. Res.-Biogeo., 111, G02016, doi:10.1029/2005JG000142, 2006. 26897, 26899

Hansen, M. C., Stehman, S. V., Potapov, P. V., Loveland, T. R., Townshend, J. R., DeFries, R. S., Pittman, K. W., Arunarwati, B., Stolle, F., Steininger, M. K., Carroll, M., and DiMiceli, C.: Humid tropical forest clearing from 2000 to 2005 quantified by using multitemporal and multiresolution remotely sensed data, P. Natl. Acad. Sci. USA, 105, 9439–9444, 2008. 26897, 26899

Hasler, N., Werth, D., and Avissar, R.: Effects of tropical deforestation on global hydroclimate: a multimodel ensemble analysis, J. Climate, 22, 1124–1141, doi:10.1175/2008JCLI2157.1, 2009. 26897, 26902, 26909

Holben, B., Eck, T., Slutsker, I., Tanre, D., Buis, J., Setzer, A., Vermote, E., Reagan, J., Kaufman, Y., Nakajima, T., Lavenu, F., Jankowiak, I., and Smirnov, A.: AERONET: a federated instrument network and data archive for aerosol characterization, Remote Sens. Environ., 66, 1–16, 1998. 26898, 26902

Huang, J., Minnis, P., Lin, B., Wang, T., Yi, Y., Hu, Y., Sun-Mack, S., and Ayers, K.: Possible influences of Asian dust aerosols on cloud properties and radiative forcing observed from MODIS and CERES, Geophys. Res. Lett., 33, L06824, doi:10.1029/2005GL024724, 2006. 26898

Huete, A., Justice, C., and Van Leeuwen, W.: MODIS vegetation index (MOD13), Algorithm theoretical basis document, 3, 213, 1999. 26901

Huete, A., Didan, K., Miura, T., Rodriguez, E. P., Gao, X., and Ferreira, L. G.: Overview of the radiometric and biophysical performance of the MODIS vegetation indices, Remote Sens. Environ., 83, 195–213, 2002. 26909

Jacobson, M. Z.: Strong radiative heating due to the mixing state of black carbon in atmospheric aerosols, Nature, 409, 695–697, 2001. 26898

Langmann, B., Duncan, B., Textor, C., Trentmann, J., and van der Werf, G. R.: Vegetation fire emissions and their impact on air pollution and climate, Atmos. Environ., 43, 107–116, 2009. 26897, 26899

Miettinen, J., Hyer, E., Chia, A. S., Kwoh, L. K., and Liew, S. C.: Detection of vegetation fires and burnt areas by remote sensing in insular Southeast Asian conditions: current status of knowledge and future challenges, Int. J. Remote Sens., 34, 4344–4366, 2013. 26899

Ming, Y., Ramaswamy, V., and Persad, G.: Two opposing effects of absorbing aerosols on global-mean precipitation, Geophys. Res. Lett., 37, L13701, doi:10.1029/2010GL042895, 2010. 26898

Myneni, R., Hoffman, S., Knyazikhin, Y., Privette, J., Glassy, J., Tian, Y., Wang, Y., Song, X., Zhang, Y., Smith, G., Lotsch, A., Friedl, M., Morisette, J. T., Votava, P., Nemani, R. R., and Running, S. W.: Global products of vegetation leaf area and fraction absorbed PAR from year one of MODIS data, Remote Sens. Environ., 83, 214–231, 2002. 26909

Myneni, R. B., Yang, W., Nemani, R. R., Huete, A. R., Dickinson, R. E., Knyazikhin, Y., Didan, K., Fu, R., Juárez, R. I. N., Saatchi, S. S., Hashimoto, H., Ichii, K., Shabanov, N. V., Tan, B., Ratana, P., Privette, J. L., Morisette, J. T., Vermote, E. F., Roy, D. P., Wolfe, R. E., Friedl, M. A., Running, S. W., Votava, P., El-Saleous, N., Devadiga, S., Su, Y., and Salomonson, V. V.: Large seasonal swings in leaf area of Amazon rainforests, P. Natl. Acad. Sci. USA, 104, 4820–4823, 2007. 26909

Nakajima, T., Higurashi, A., Takeuchi, N., and Herman, J. R.: Satellite and ground-based study of optical properties of 1997 Indonesian forest Fire aerosols, Geophys. Res. Lett., 26, 2421–2424, 1999. 26897

Neale, R. and Slingo, J.: The maritime continent and its role in the global climate: a GCM study, J. Climate, 16, 834–848, 2003. 26898

Nightingale, J., Nickeson, J., Justice, C., Baret, F., Garrigues, S., Wolfe, R., and Masuoka, E.: Global validation of EOS land products, lessons learned and future challenges: a MODIS case study, in: Proceedings of 33rd International Symposium on Remote Sensing of Environment: Sustaining the Millennium Development Goals, Stresa, Italy, available at: http://landval.gsfc.nasa.gov/pdf/ISRSE_Nightingale.pdf (last access: 1 June 2015), p. 4, 2008. 26901

Petrenko, M., Kahn, R., Chin, M., Soja, A., Kucsera, T., and Harshvardhan: The use of satellite-measured aerosol optical depth to constrain biomass burning emissions source strength in the global model GOCART, J. Geophys. Res.-Atmos., 117, D18212, doi:10.1029/2012JD017870, 2012. 26898, 26899

Phillips, O. L., Van der Heijden, G., Lewis, S. L., López-González, G., Aragão, L. E., Lloyd, J., Malhi, Y., Monteagudo, A., Almeida, S., Dávila, E. A., Amaral, I., Andelman, S., Andrade,

ACPD
15, 26895–26957, 2015

CC BY

A., Arroyo, L., Aymard, G., Baker, T. R., Blanc, L., Bonal, D., de Oliveira, A. C., Chao, K. J., Cardozo, N. D., da Costa, L., Feldpausch, T. R., Fisher, J. B., Fyllas, N. M., Freitas, M. A., Galbraith, D., Gloor, E., Higuchi, N., Honorio, E., Jiménez, E., Keeling, H., Killeen, T. J., Lovett, J. C., Meir, P., Mendoza, C., Morel, A., Vargas, P. N., Patiño, S., Peh, K. S., Cruz, A. P., Prieto, A., Quesada, C. A., Ramírez, F., Ramírez, H., Rudas, A., Salamão, R., Schwarz, M., Silva, J., Silveira, M., Slik, J. W., Sonké, B., Thomas, A. S., Stropp, J., Taplin, J. R., Vásquez, R., and Vilanova, E.: Drought–mortality relationships for tropical forests, New Phytol., 187, 631–646, 2010. 26905, 26909

Podgorny, I., Li, F., and Ramanathan, V.: Large aerosol radiative forcing due to the 1997 Indonesian forest fire, Geophys. Res. Lett., 30, 1028, doi:10.1029/2002GL015979, 2003. 26897, 26915

Ramanathan, V. and Carmichael, G.: Global and regional climate changes due to black carbon, Nat. Geosci., 1, 221–227, 2008. 26898

Reid, J. S., Hyer, E. J., Johnson, R. S., Holben, B. N., Yokelson, R. J., Zhang, J., Campbell, J. R., Christopher, S. A., Di Girolamo, L., Giglio, L., Holz, R. E., Kearney, C., Miettinen, J., Reid, E. A., Turk, F. J., Wang, J., Xian, P., Zhao, G., Balasubramanian, R., Ning Chew, B., Janjai, S., Lagrosas, N., Lestari, P., Lin, N.-H., Mahmud, M., Nguyen, A. X., Norris, B., Oanh, N. T. K., Oo, M., Salinas, S. V., Judd, E., Welton, and Chin Liew, S.: Observing and understanding the Southeast Asian aerosol system by remote sensing: an initial review and analysis for the Seven Southeast Asian Studies (7SEAS) program, Atmos. Res., 122, 403–468, 2013. 26897

Remer, L. A., Kaufman, Y., Tanré, D., Mattoo, S., Chu, D., Martins, J. V., Li, R.-R., Ichoku, C., Levy, R., Kleidman, R., Eck, T. F., Vermote, E., and Holben, B. N.: The MODIS aerosol algorithm, products, and validation, J. Atmos. Sci., 62, 947–973, 2005. 26900

Remer, L. A., Mattoo, S., Levy, R. C., and Munchak, L. A.: MODIS 3 km aerosol product: algorithm and global perspective, Atmos. Meas. Tech., 6, 1829–1844, doi:10.5194/amt-6-1829-2013, 2013. 26899

Rosenfeld, D.: TRMM observed first direct evidence of smoke from forest fires inhibiting rainfall, Geophys. Res. Lett., 26, 3105–3108, 1999. 26897

Shi, Y., Zhang, J., Reid, J. S., Hyer, E. J., Eck, T. F., Holben, B. N., and Kahn, R. A.: A critical examination of spatial biases between MODIS and MISR aerosol products – application for potential AERONET deployment, Atmos. Meas. Tech., 4, 2823–2836, doi:10.5194/amt-4-2823-2011, 2011. 26921

CC BY

Tao, W.-K., Chen, J.-P., Li, Z., Wang, C., and Zhang, C.: Impact of aerosols on convective clouds and precipitation, Rev. Geophys., 50, RG2001, doi:10.1029/2011RG000369, 2012. 26898

Taylor, D.: Biomass burning, humans and climate change in Southeast Asia, Biodivers. Conserv., 19, 1025–1042, doi:10.1007/s10531-009-9756-6, 2010. 26897, 26908, 26909

Tipayarom, D. and Oanh, N. K.: Effects from open rice straw burning emission on air quality in the Bangkok Metropolitan Region, Science Asia, 33, 339–345, 2007. 26908

van der Werf, G. R., Randerson, J. T., Giglio, L., Collatz, G. J., Kasibhatla, P. S., and Arellano Jr., A. F.: Interannual variability in global biomass burning emissions from 1997 to 2004, Atmos. Chem. Phys., 6, 3423–3441, doi:10.5194/acp-6-3423-2006, 2006. 26897, 26899

van der Werf, G. R., Dempewolf, J., Trigg, S. N., Randerson, J. T., Kasibhatla, P. S., Giglio, L., Murdiyarso, D., Peters, W., Morton, D. C., Collatz, G. J., Dolman, A. J., and DeFries, R. S.: Climate regulation of fire emissions and deforestation in equatorial Asia, P. Natl. Acad. Sci. USA, 105, 20350–20355, doi:10.1073/pnas.0803375105, 2008. 26897

Wang, C.: Impact of direct radiative forcing of black carbon aerosols on tropical convective precipitation, Geophys. Res. Lett., 34, L05709, doi:10.1029/2006GL028416, 2007. 26898

Wang, C.: Impact of anthropogenic absorbing aerosols on clouds and precipitation: a review of recent progresses, Atmos. Res., 122, 237–249, 2013. 26898

Wohl, E., Barros, A., Brunsell, N., Chappell, N. A., Coe, M., Giambelluca, T., Goldsmith, S., Harmon, R., Hendrickx, J. M., Juvik, J., McDonnell, J., and Ogden, F.: The hydrology of the humid tropics, Nature Climate Change, 2, 655–662, 2012. 26905

Wooster, M. J., Perry, G. L. W., and Zoumas, A.: Fire, drought and El Niño relationships on Borneo (Southeast Asia) in the pre-MODIS era (1980–2000), Biogeosciences, 9, 317–340, doi:10.5194/bg-9-317-2012, 2012. 26897, 26898, 26909

Yang, W., Tan, B., Huang, D., Rautiainen, M., Shabanov, N. V., Wang, Y., Privette, J. L., Huemmrich, K. F., Fensholt, R., Sandholt, I., Weiss, M., Ahl, D. E., Gower, S. T., Nemani, R. R., Knyazikhin, Y., and Myneni, R. B.: MODIS leaf area index products: from validation to algorithm improvement, IEEE T. Geosci. Remote, 44, 1885–1898, 2006. 26901

ACPD
15, 26895–26957, 2015

Estimating AOD from meteorology and land-use over Southeast Asia

J. B. Cohen and E. Lecoeur

CC BY

Table 1. Characteristics of the MODIS and TRMM data used in this study.

Variable	Data set origin	Horizontal resolution	Temporal resolution
AOD	MODIS08_E3[1]	$1^\circ \times 1^\circ$	8-day
LAI	MODIS15_A2[2]	1 km	8-day
NDVI	MODIS13_A2[2]	1 km	16-day
FireMask	MODIS14_A2[2]	1 km	8-day
Precipitation	TRMM 3B42[3]	$0.25^\circ \times 0.25^\circ$	daily

[1] http://modis-atmos.gsfc.nasa.gov/MOD08_E3/
[2] http://modis.gsfc.nasa.gov/data/dataprod/dataproducts.php?MOD_NUMBER=15
[3] http://disc.sci.gsfc.nasa.gov/precipitation/documentation/TRMM_README/TRMM_3B42_readme.shtml

ACPD
15, 26895–26957, 2015

CC BY

Table 2. Average error and correlation between AOD at 0.55 µm from MODIS and 8 reconstructed AOD with different thresholds: τ = P90(PC), τ = P87.5(PC), τ = P83.5(PC), and τ = P75(PC) on the northern and southern regions, obtained by using Eqs. (6) and (7).

Region	τ = P90(PC)		τ = P87.5(PC)		τ = P83.5(PC)		τ = P75(PC)	
	Err	Corr(%)	Err	Corr(%)	Err	Corr(%)	Err	Corr(%)
North (w FireMask)	−0.02	76	−0.02	78	−0.02	80	**−0.01**	**83**
North (w/o FireMask)	−0.02	69	−0.02	70	−0.02	71	−0.02	71
South (w FireMask)	−0.01	77	**−0.01**	**78**	−0.01	75	0.01	69
South (w/o FireMask)	−0.01	71	−0.01	70	−0.01	66	−0.01	57

ACPD
15, 26895–26957, 2015

Estimating AOD from meteorology and land-use over Southeast Asia

J. B. Cohen and E. Lecoeur

CC BY

Table 3. Complementary information on AERONET stations: geographical location, data availability, average (μ) and standard deviation (σ) values for AOD, LAI, and NDVI from MODIS, and environment description.

Stations	Availability	AOD	LAI	NDVI	Other information
Bac Giang, VN (North)	2003–2009	$\mu = 0.57$ $\rho = 0.28$	$\mu = 0.68$ $\rho = 0.43$	$\mu = 0.45$ $\rho = 0.15$	Rural, surrounded by crops and industrial parks
Chiang Mai, TH (North)	2006–2013	$\mu = 0.29$ $\rho = 0.17$	$\mu = 2.19$ $\rho = 0.77$	$\mu = 0.61$ $\rho = 0.07$	Urban, surrounded by agricultural fields
Mukdahan, TH (North)	2003–2009	$\mu = 0.32$ $\rho = 0.16$	$\mu = 1.13$ $\rho = 0.37$	$\mu = 0.55$ $\rho = 0.09$	Rural, surrounded by agricultural fields
Nghia Do, VN (North)	2010–2013	$\mu = 0.57$ $\rho = 0.29$	$\mu = 0.92$ $\rho = 0.59$	$\mu = 0.42$ $\rho = 0.15$	Urban
Pimai, TH (North)	2003–2007	$\mu = 0.33$ $\rho = 0.17$	$\mu = 0.72$ $\rho = 0.27$	$\mu = 0.49$ $\rho = 0.1$	Rural, surrounded by agricultural fields
Ubon Ratchathani, TH (North)	2009–2012	$\mu = 0.33$ $\rho = 0.17$	$\mu = 1.03$ $\rho = 0.33$	$\mu = 0.52$ $\rho = 0.07$	Semi-urban, surrounded by agricultural fields
Vientiane, LA (North)	2011–2012	$\mu = 0.35$ $\rho = 0.21$	$\mu = 2.03$ $\rho = 0.45$	$\mu = 0.55$ $\rho = 0.08$	Semi-urban, surrounded by agricultural fields
Jambi, ID (South)	2012–2013	$\mu = 0.36$ $\rho = 0.31$	$\mu = 2.72$ $\rho = 1.48$	$\mu = 0.66$ $\rho = 0.11$	Rural, surrounded by jungle
Kuching, MY (South)	2011–2013	$\mu = 0.31$ $\rho = 0.32$	$\mu = 3.75$ $\rho = 1.65$	$\mu = 0.7$ $\rho = 0.1$	Rural, surrounded by jungle
Palangkaraya, ID (South)	2012–2013	$\mu = 0.3$ $\rho = 0.37$	$\mu = 3.21$ $\rho = 1.43$	$\mu = 0.69$ $\rho = 0.11$	Rural, surrounded by jungle
Singapore, SG (South)	2006–2013	$\mu = 0.34$ $\rho = 0.25$	$\mu = 2.38$ $\rho = 1.29$	$\mu = 0.42$ $\rho = 0.06$	Urban

VN stands for Vietnam, TH for Thailand, LA for Laos, ID for Indonesia, MY for Malaysia, and SG for Singapore.

Discussion Paper | Discussion Paper | Discussion Paper | Discussion Paper |

CC BY

Table 4. Beginning and ending of the annual peak of high AOD over the northern region during the 2001–2013 periods.

Years	Bac Giang	Chiang Mai	Mukdahan	Nghia Do	Pimai	Ubon	Vientiane
2001	Feb–May	Feb–Apr	Feb–Mar	Jan–May	Feb–Mar	Feb–Mar	Feb–Apr
2002	Feb–Apr	Mar–Apr	Feb–Mar	Feb–Apr	Feb–Apr	Feb–Apr	Feb–Apr
2003	Apr–Jun	Mar–Apr	Mar–Mar	Feb–Jun	Feb–Apr	Mar–Apr	Mar–Apr
2004	Feb–Jun	Feb–Apr	Feb–Apr	Jan–Jun	Feb–Apr	Feb–Apr	Feb–Apr
2005	Feb–Mar	Mar–Apr	Feb–May	Feb–Apr	Feb–Apr	Feb–Apr	Feb–Apr
2006	Feb–Apr	Mar–Apr	Mar–Apr	Feb–May	Feb–Apr	Feb–Apr	Feb–Apr
2007	Jan–Apr	Feb–Apr	Feb–Apr	Jan–May	Jan–Mar	Feb–Mar	Jan–Apr
2008	Feb–May	Mar–May	Feb–Apr	Feb–May	Feb–Mar	Feb–Apr	Feb–Apr
2009	Feb–May	Feb–Apr	Feb–Mar	Feb–May	Feb–Mar	Feb–Mar	Feb–May
2010	Feb–May	Mar–May	Feb–Apr	Feb–May	Feb–Apr	Feb–Apr	Feb–May
2011	Jan–May	Apr–Apr	Feb–Apr	Feb–Jun	Feb–Apr	Feb–Apr	Feb–Apr
2012	Feb–Apr	Mar–Apr	Feb–Apr	Feb–May	Feb–Apr	Feb–Apr	Feb–Apr
2013	Feb–May	Mar–Apr	Mar–Mar	Feb–May	Feb–Apr	Feb–Apr	Feb–Apr

ACPD
15, 26895–26957, 2015

CC BY

Table 5. Average values of maximum AOD and average LAI and NDVI during the two annual AOD peaks over the northern region for the 2001–2013 period.

Stations	Maximum AOD		Average LAI		Average NDVI	
	1st Peak	2nd Peak	1st Peak	2nd Peak	1st Peak	2nd Peak
Bac Giang	0.89	0.74	0.44	1.1	0.37	0.58
Chiang Mai	0.5	0.4	2.3	2.97	0.56	0.7
Mukdahan	0.53	0.44	0.96	1.62	0.45	0.67
Nghia Do	0.9	0.71	0.87	1.45	0.39	0.54
Pimai	0.5	0.46	0.54	1.22	0.42	0.61
Ubon R	0.51	0.46	1.09	1.14	0.48	0.55
Vientiane	0.62	0.59	2.13	2.39	0.52	0.63

ACPD
15, 26895–26957, 2015

J. B. Cohen and E. Lecoeur

CC BY

Table 6. Statistics over the northern region compared to the AERONET stations. Overlapped periods between AOD_{REC}^{North} and AERONET are stated in parenthesis.

Stations	AOD_{MODIS} Err	AOD_{MODIS} Corr (%)	AOD_{REC}^{North} Err	AOD_{REC}^{North} Corr (%)
Chiang Mai (218/598)	−0.1	83	−0.1	75
Bac Giang (154/598)	−0.03	74	−0.06	42
Mukdahan (238/598)	−0.01	79	−0.01	69
Nghia Do (79/598)	−0.12	74	−0.14	42
Pimai (120/598)	0	77	−0.01	57
Ubon Ratchathani (99/598)	−0.01	88	−0.02	61
Vientiane (36/598)	−0.08	83	−0.07	64

* Not statistically significant at the $p = 0.05$ level.

ACPD
15, 26895–26957, 2015

Estimating AOD from meteorology and land-use over Southeast Asia

J. B. Cohen and E. Lecoeur

CC BY

Table 7. Statistics over the northern region compared to the AERONET stations during fire periods. Overlapped periods between AOD_{REC}^{North} and AERONET are stated in parenthesis.

Stations	AOD_{MODIS}		AOD_{REC}^{North}	
	Err	Corr (%)	Err	Corr (%)
Chiang Mai (62/151)	−0.26	91	−0.26	64
Bac Giang (46/151)	−0.07	75	−0.24	33
Mukdahan (74/151)	−0.08	86	−0.15	49
Nghia Do (15/151)	−0.08	75	−0.5	62
Pimai (45/151)	−0.03	75	−0.12	43
Ubon Ratchathani (23/151)	−0.07	88	−0.22	80
Vientiane (8/151)	−0.14	93	−0.33	92

* Not statistically significant at the $p = 0.05$ level.

ACPD
15, 26895–26957, 2015

Estimating AOD from meteorology and land-use over Southeast Asia

J. B. Cohen and E. Lecoeur

CC BY

Table 8. Average values of maximum AOD and average LAI and NDVI during the annual AOD peak over the southern region for the 2001–2013 period.

Stations	Maximum AOD	Average LAI	Average NDVI
Jambi	0.98	2.92	0.68
Kuching	0.66	4.16	0.75
Palangkaraya	1.05	3.72	0.68
Singapore	0.87	1.71	0.4

ACPD
15, 26895–26957, 2015

Estimating AOD from meteorology and land-use over Southeast Asia

J. B. Cohen and E. Lecoeur

CC BY

Table 9. Beginning and ending of the annual peak of high AOD over the southern region during the 2001–2013 period.

Years	Jambi	Kuching	Palangkaraya	Singapore
2001	Aug–Sep	Aug–Sep	Aug–Sep	Aug–Aug
2002	Aug–Nov	Aug–Nov	Aug–Nov	Aug–Nov
2003	Sep–Oct	Sep–Oct	Oct–Oct	Sep–Sep
2004	Aug–Nov	Aug–Oct	Aug–Oct	Aug–Oct
2005	Aug–Sep	Aug–Sep	Aug–Sep	Aug–Sep
2006	Aug–Nov	Aug–Nov	Aug–Nov	Aug–Nov
2007	Sep–Oct	Sep–Oct	Sep–Oct	Sep–Oct
2008	Aug–Aug	–	–	–
2009	Sep–Oct	Aug–Oct	Aug–Oct	Sep–Oct
2010	–	–	–	–
2011	Aug–Sep	Aug–Sep	Aug–Sep	Aug–Sep
2012	Sep–Oct	Sep–Oct	Sep–Oct	Sep–Oct
2013	–	–	Sep–Sep	Sep–Sep

ACPD
15, 26895–26957, 2015

CC BY

Table 10. Statistics over the southern region compared to the AERONET stations. Overlapped periods between AOD_{REC}^{South} and AERONET are stated in parenthesis.

Stations	AOD_{MODIS}		AOD_{REC}^{South}	
	Err	Corr (%)	Err	Corr (%)
Jambi (64/598)	−0.12	51	−0.26	76
Kuching (91/598)	0.06	75	0.13	66
Palangkaraya (65/598)	−0.11	71	−0.11	74
Singapore (279/598)	−0.02	29	0.01	44

* Not statistically significant at the $p = 0.05$ level.

ACPD
15, 26895–26957, 2015

Estimating AOD from meteorology and land-use over Southeast Asia

J. B. Cohen and E. Lecoeur

CC BY

Table 11. Statistics over the southern region compared to the AERONET stations during fire periods. Overlapped periods between AOD_{REC}^{South} and AERONET are stated in parenthesis.

Stations	AOD_{MODIS}		AOD_{REC}^{South}	
	Err	Corr (%)	Err	Corr (%)
Jambi (6/74)	−0.51	80*	−0.54	71*
Kuching (10/74)	−0.28	80	−0.03	−9*
Palangkaraya (6/74)	−0.5	85	−0.45	31*
Singapore (24/74)	−0.23	−21*	−0.09	8*

* Not statistically significant at the $p = 0.05$ level.

Discussion Paper | Discussion Paper | Discussion Paper | Discussion Paper |

ACPD
15, 26895–26957, 2015

J. B. Cohen and E. Lecoeur

Table 12. Error and correlation between the reconstructed AOD vs. AERONET and MISR on a monthly basis over the northern region for the whole 2001–2013 period. Overlapped periods between AOD_{REC}^{South} and AERONET, on one hand, and between AOD_{REC}^{South} and MISR on the other hand, are stated in parenthesis.

Stations	AERONET		MISR	
	Err	Corr (%)	Err	Corr (%)
Chiang Mai (65/156)–(129/156)	−0.09	82	0.02	77
Bac Giang (49/156)–(127/156)	−0.03	73	0.1	72
Mukdahan (72/156)–(135/156)	0	78	0.04	79
Nghia Do (28/156)–(133/156)	−0.12	83	0.07	71
Pimai (41/156)–(145/156)	0.02	70	0.03	66
Ubon Ratchathani (32/156)–(136/156)	0	90	0.05	74
Vientiane (15/156)–(127/156)	−0.01	76	0.02	81

* Not statistically significant at the $p = 0.05$ level.

ACPD
15, 26895–26957, 2015

Table 13. Same as Table 12 over the southern region.

Stations	AERONET		MISR	
	Err	Corr (%)	Err	Corr (%)
Jambi (18/156)–(79/156)	−0.14	57	0.06	69
Kuching (25/156)–(114/156)	−0.06	71	0.1	64
Palangkaraya (18/156)–(102/156)	−0.11	73	0.04	79
Singapore (78/156)–(122/156)	−0.11	−2*	0.04	57

* Not statistically significant at the $p = 0.05$ level.

ACPD
15, 26895–26957, 2015

Estimating AOD from meteorology and land-use over Southeast Asia

J. B. Cohen and E. Lecoeur

CC BY

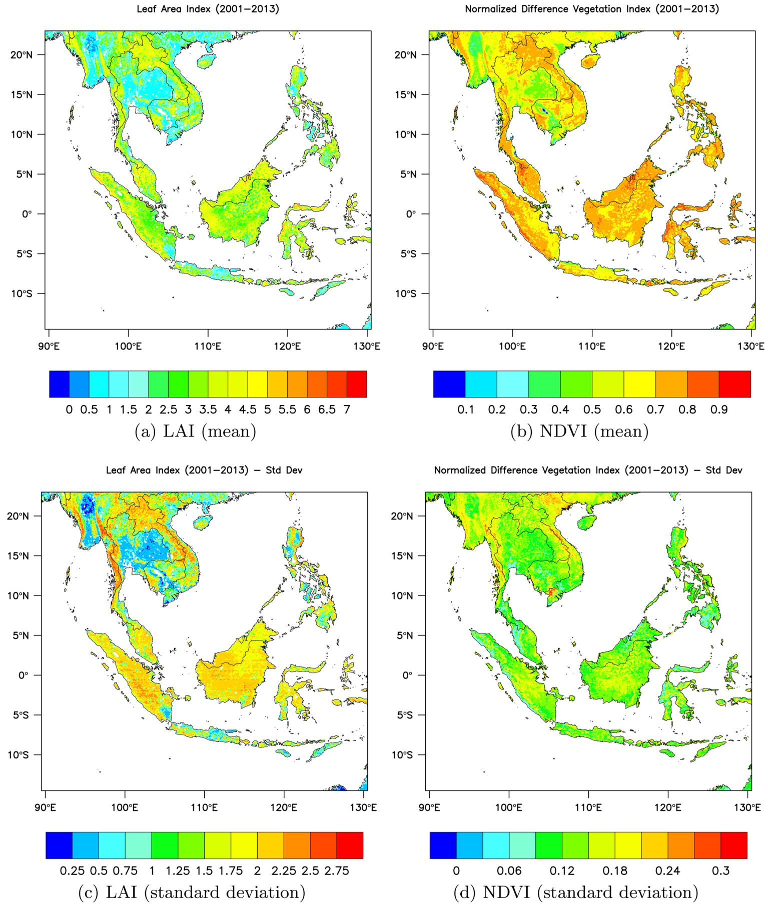

Figure 1. Climatological values of LAI (first column) and NDVI (second column) for the 2001–2013 period. Average values are displayed on the first line, while the standard deviation is displayed on the second line.

ACPD
15, 26895–26957, 2015

Estimating AOD from meteorology and land-use over Southeast Asia

J. B. Cohen and E. Lecoeur

Title Page
Abstract | Introduction
Conclusions | References
Tables | Figures
◀| |▶
◀ ▶
Back | Close
Full Screen / Esc
Printer-friendly Version
Interactive Discussion

CC BY

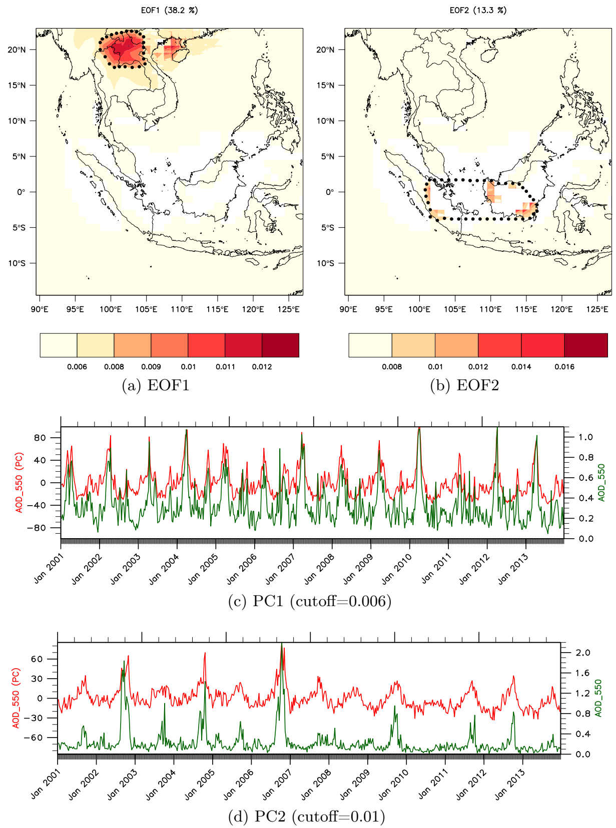

Figure 2. First line: EOF1 **(a)** and EOF2 **(b)** of the AOD (2001–2013). Regions of highest AOD variability are delineated by black dots. Second line: PC1 **(c)** (red curve) and their associated AOD (green curve) averaged on the region. Third line: PC2 **(d)** (red curve) and their associated AOD (green curve) averaged on the region.

ACPD
15, 26895–26957, 2015

J. B. Cohen and E. Lecoeur

CC BY

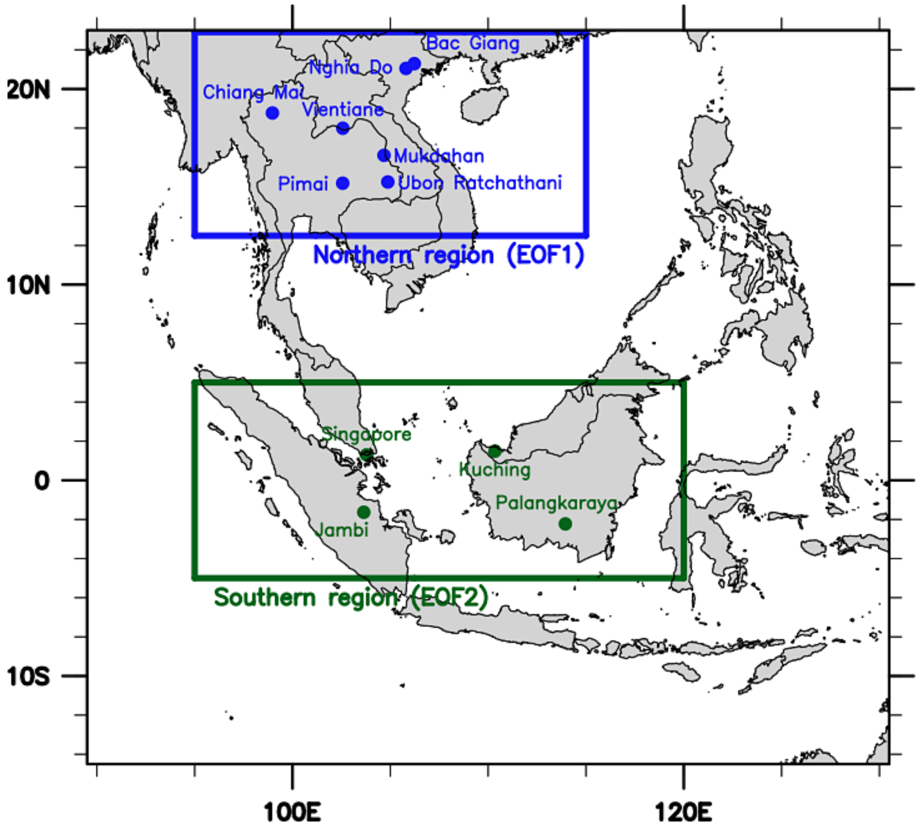

Figure 3. Domain with the two EOF regions highlighted and the location of the AERONET stations.

ACPD
15, 26895–26957, 2015

Estimating AOD from meteorology and land-use over Southeast Asia

J. B. Cohen and E. Lecoeur

Title Page
Abstract | Introduction
Conclusions | References
Tables | Figures
Back | Close
Full Screen / Esc
Printer-friendly Version
Interactive Discussion

CC BY

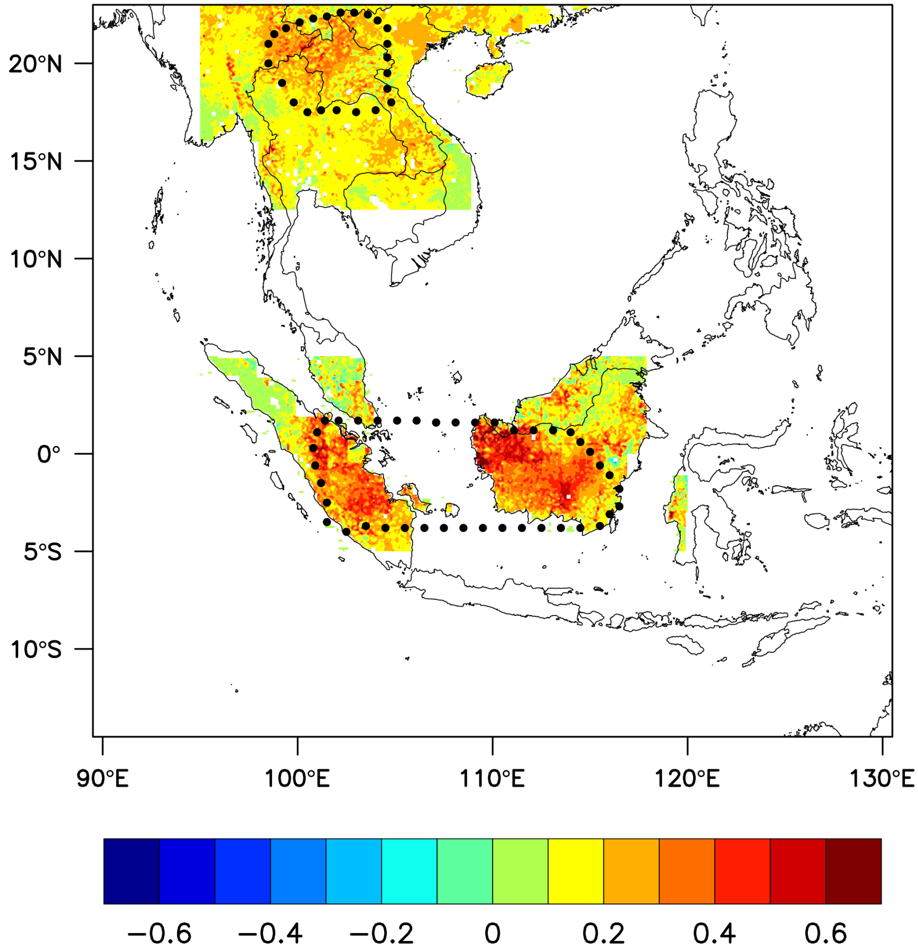

Figure 4. Regression Coefficients (δ_1) associated to FireMask for Eq. (6). Regions of highest AOD variability from the EOF analysis are delineated by black dots.

ACPD
15, 26895–26957, 2015

CC BY

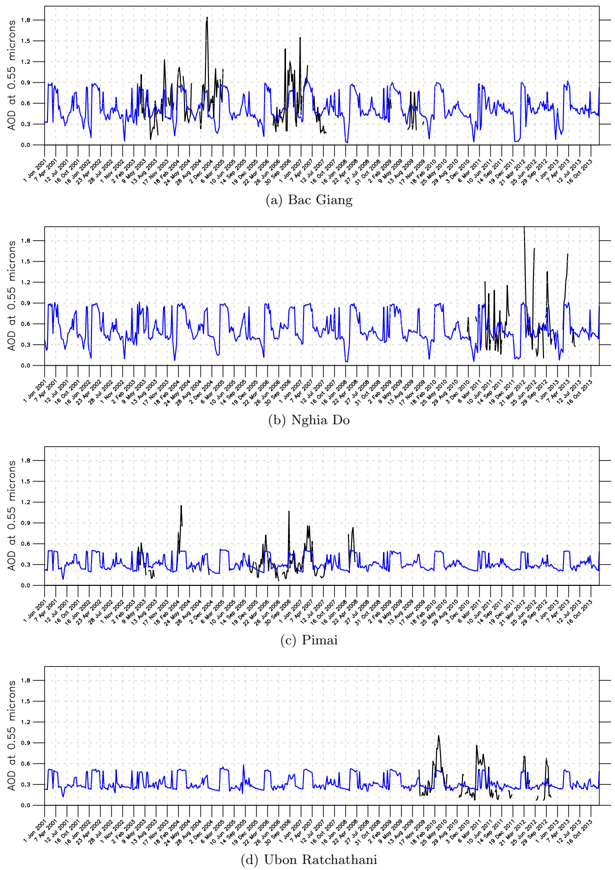

Figure 5. Temporal series of 8-day AERONET AOD (black) and AOD^{North}_{REC} (blue) at Bac Giang **(a)**, Nghia Do **(b)**, Pimai **(c)**, and Ubon Ratchathani **(d)** (2001–2013).

ACPD
15, 26895–26957, 2015

CC BY

ACPD
15, 26895–26957, 2015
Estimating AOD from meteorology and land-use over Southeast Asia
J. B. Cohen and E. Lecoeur

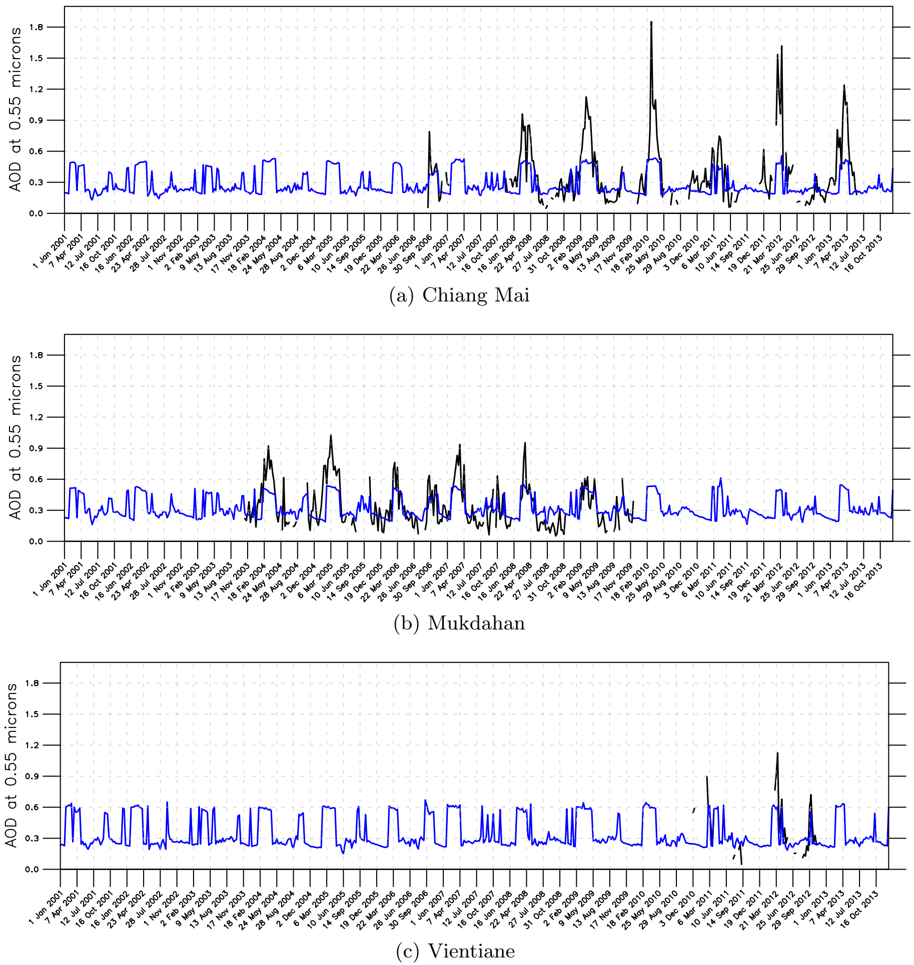

Figure 6. Temporal series of 8-day AERONET AOD (black) and AOD^{North}_{REC} (blue) at Chiang Mai **(a)**, Mukdahan **(b)**, and Vientiane **(c)** (2001–2013).

CC BY

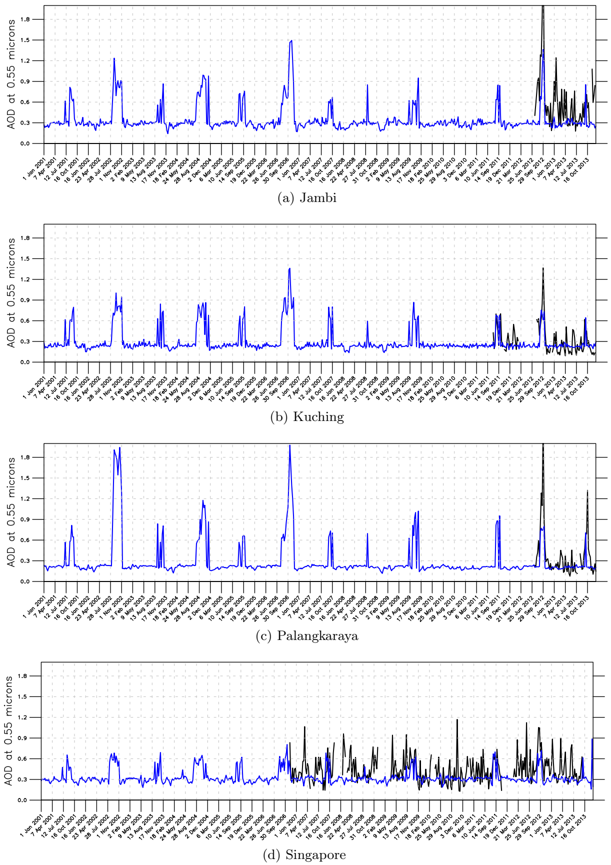

Figure 7. Temporal series of 8-day AERONET AOD (black) and AOD^{South}_{REC} (blue) at Jambi **(a)**, Kuching **(b)**, Palangkaraya **(c)**, and Singapore **(d)** (2001–2013).

ACPD
15, 26895–26957, 2015

CC BY

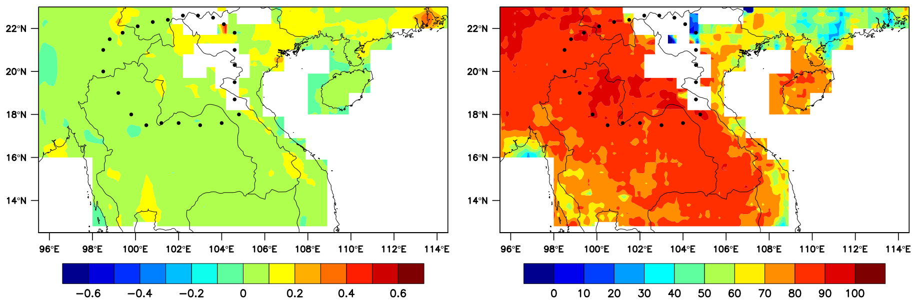

(a) Mean error (b) Correlation

Figure 8. Basic statistics between MISR and AOD_{REC}^{North} on a monthly basis (2001–2013). Regions of highest AOD variability from the EOF analysis are delineated by black dots. Within these dots, the mean correlation is 84.8 %, while it is 77.3 % in average (the mean errors are 0.06 in both cases).

ACPD
15, 26895–26957, 2015
Estimating AOD from meteorology and land-use over Southeast Asia
J. B. Cohen and E. Lecoeur

CC BY

Discussion Paper | Discussion Paper | Discussion Paper | Discussion Paper |

ACPD

15, 26895–26957, 2015

Estimating AOD from meteorology and land-use over Southeast Asia

J. B. Cohen and E. Lecoeur

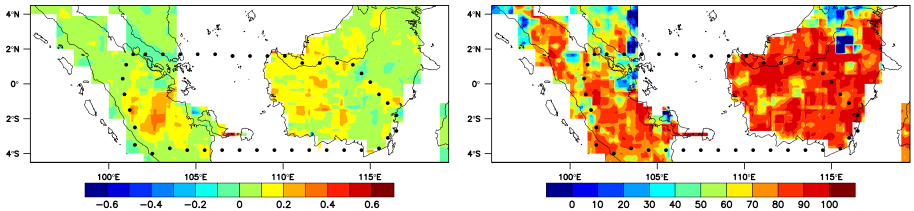

(a) Mean error (b) Correlation

Figure 9. Basic statistics between MISR and AOD_{REC}^{South} on a monthly basis (2001–2013). Regions of highest AOD variability from the EOF analysis are delineated by black dots. Within these dots, the mean correlation is 79.2 %, while it is 72.4 % in average (the mean errors are 0.08 in both cases).

CC BY

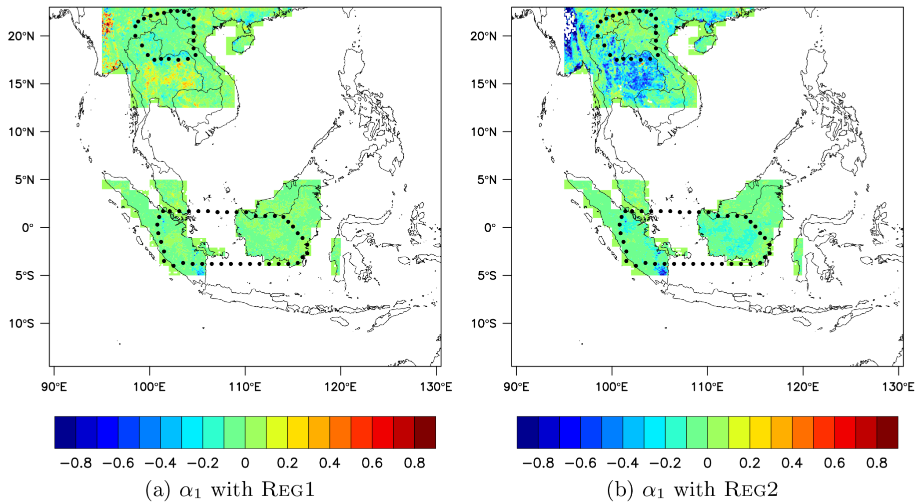

Figure A1. Regression Coefficients associated to LAI for Eq. (6) **(a)** and Eq. (7) **(b)**.

ACPD
15, 26895–26957, 2015

Estimating AOD from meteorology and land-use over Southeast Asia

J. B. Cohen and E. Lecoeur

CC BY

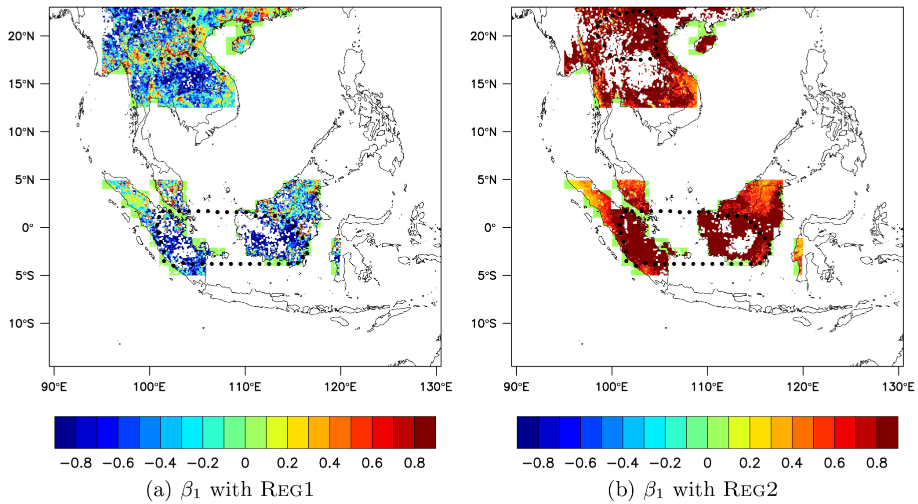

Figure A2. Regression Coefficients associated to NDVI for Eq. (6) **(a)** and Eq. (7) **(b)**.

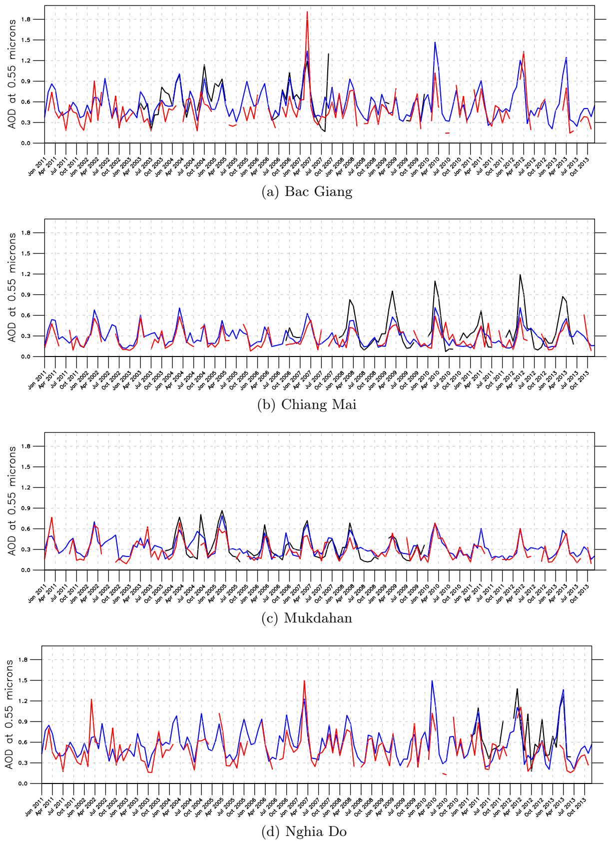

Figure B1. Temporal series of AERONET AOD (black), AOD_{REC}^{North} (blue), and AOD from MISR (red) at four stations of the northern region (2001–2013).

ACPD
15, 26895–26957, 2015

CC BY

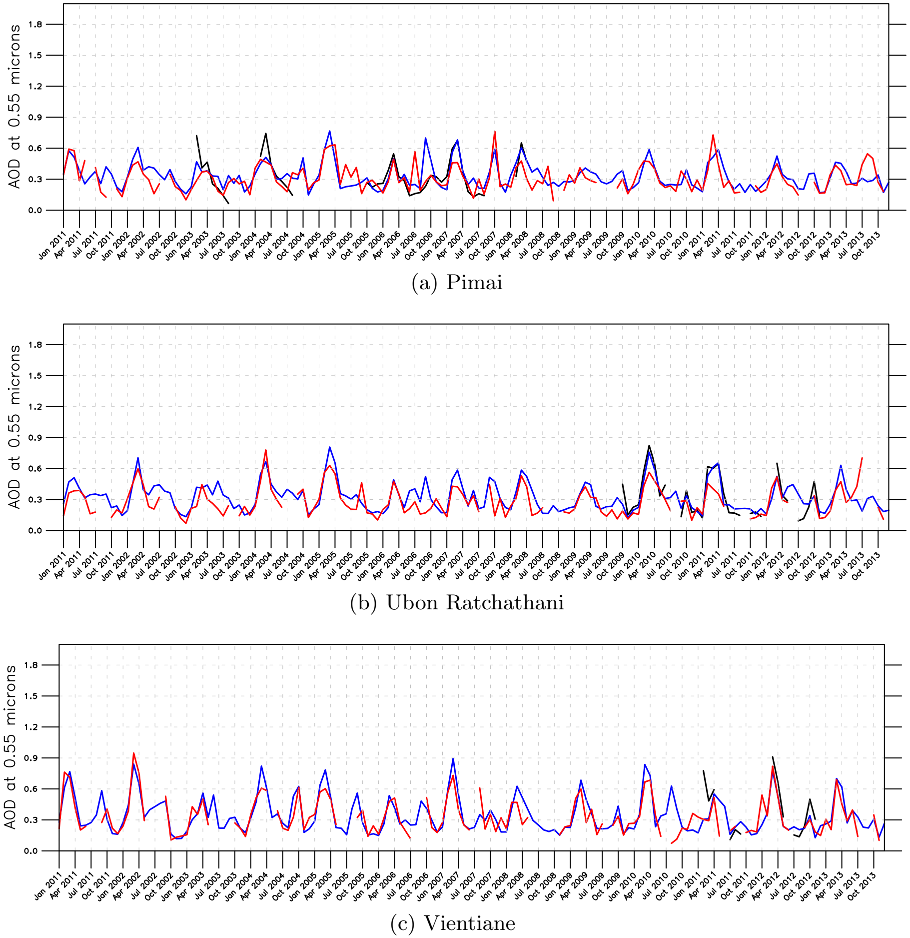

Figure B2. Temporal series of AERONET AOD (black), AOD_{REC}^{North} (blue), and AOD from MISR (red) at three stations of the northern region (2001–2013).

ACPD
15, 26895–26957, 2015

Estimating AOD from meteorology and land-use over Southeast Asia

J. B. Cohen and
E. Lecoeur

Title Page
Abstract | Introduction
Conclusions | References
Tables | Figures
◀| |▶
◀ ▶
Back | Close
Full Screen / Esc
Printer-friendly Version
Interactive Discussion

CC BY

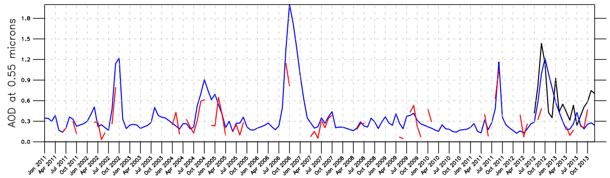

(a) Jambi

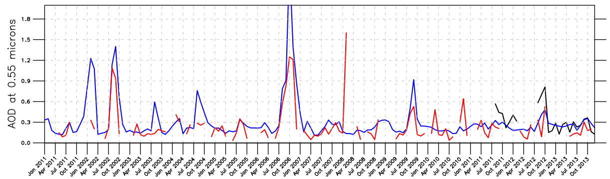

(b) Kuching

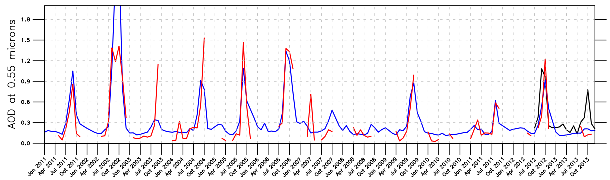

(c) Palangkaraya

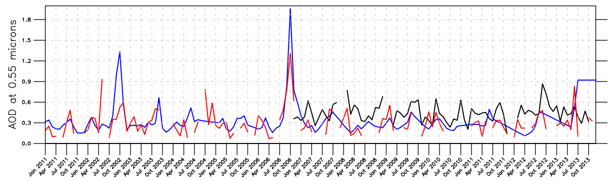

(d) Singapore

Figure B3. Temporal series of AERONET AOD (black), AOD_{REC}^{North} (blue), and AOD from MISR (red) at two stations of the southern region (2001–2013).